Effect of Pressure on Electronic Structure and Transport of Chalcogenides (ZrSiS and PbTe)

A Thesis

Submitted in partial fulfillment for the Degree of

MASTER OF SCIENCE

as a part of Integrated Pn. D. programme in

MATERIALS SCIENCE

by

Shashank Chaturvedi

CHEMISTRY AND PHYSICS OF MATERIALS UNIT

JAWAHARLAL NEHRU CENTRE FOR ADVANCED SCIENTIFIC RESEARCH

BANGLORE - 560 064

MARCH 2019

Dedicated to all those who believe. . .

DECLARATION

I hereby declare that the matter embodied in the thesis entitled " **Effect of Pressure on Electronic Structure and Transport of Chalcogenides (ZrSiS and PbTe)**" is the result of investigations carried out by me at the Chemistry and Physics of Materials Unit, Jawaharlal Nehru Centre for Advanced Scientific Research, Bangalore, India under the supervision of Prof. Umesh V. Waghmare and that it has not been submitted elsewhere for the award of any degree or diploma.

In keeping with the general practice in reporting scientific observations, due acknowledgement has been made whenever the work described is based on the findings of other investigators.

Shashank Chaturvedi

CERTIFICATE

I hereby declare that the matter embodied in the thesis entitled "**Effect of Pressure on Electronic Structure and Transport of chalcogenides (ZrSiS and PbTe)**" is the result of investigations carried out by Mr. Shashank Chaturvedi at the Chemistry and Physics of Materials Unit, Jawaharlal Nehru Centre for Advanced Scientific Research, Bangalore, India under the supervision of Prof. Umesh V. Waghmare and that it has not been submitted elsewhere for the award of any degree or diploma. In keeping with the general practice in reporting scientific observations, due acknowledgement has been made whenever the work described is based on the findings of other investigators.

Prof. Umesh V. Waghmare

(Research Supervisor)

Acknowledgment

First of all I want to thank my research supervisor Prof. Umesh V. Waghmare for giving me the opportunity to work with him and for encouraging me always. I enjoyed to work under his supervision and his constant guidance and motivation helped me to be on the right track. I am again thankful to my supervisor for providing me the opprtunity to work with him.

I am very grateful to all the members of the Materials Theory Group who helped me in many ways during this project and in fact I have learned a lot from seniors and past and present members of the group like Meha, Suchitra, Pawan, Lakshay, Narendra, Rajendra, Koyendrila, Raagya, shivani. I had invaluable discussions about life and science with Dr. Prasad and Dr. Sampath. The life outside the lab was made enjoyable by the good presence of my colorful and enthusiastic Integrated Ph.D. batch-mates Nijita, Ashutosh, Amit, Tarandeep, Raagya, Pragya, Brijesh and Shivani. I have been benefitted a lot from them during the coursework as well as during my leisure time. I also owe a lot to the senior Ph.D. and Integrated Ph.D. students Anand, Momin, Monis, Navneet, Manodeep, Rohit, Ankit, Surishi, Divya, Janaky, Manaswee whose help (or advices) made both my academic and non-academic life a memorable and a comfortable one here at JNC.

I am highly indebted to Prof. S. Balasubramanian, Prof. A. Sundaresan, Prof. Sarit S. Agasti, Prof. C. Narayana, Prof. K. S. Narayan, Dr. R. Ganapathy, Dr. R. Datta, Prof. T. K. Maji, Prof. M. Eswaramoorthy, Prof. S. Narasimhan, Prof. U. V. Waghmare, Prof. Subir K. Das, Prof. Swapan K. Pati, Prof. T.N. Guru Row(IISc) and Prof.

A. Chakraborty (IISc) whose classes during the coursework greatly helped me in my research. Being very nice to the students, it's always been a great pleasure to discuss with them about any scientific and non-scientific issues.I want to thank our collaborators Prof. Prabhat Mandal and his student Ratnadwip from the Saha Institute of Nuclear Physics, Kolkata and Yevgeny Rakita from Weizmann Institute of Science, Israel.

I have learned a lot whenever we had any discussion with them. I convey deepest respect to my high school teachers who always inspired and motivated me to pursue higher studies. My sincere thanks also go to my childhood friends Ritam, Titu, Bantu, Pushkar and Shantanu with whom I spent the first best fifteen years of my life. I also want to thank Ritu, Ajinkya, Avi and Smriti for their support. Finally, it will be an incomplete task if I forget to acknowledge my parents. It's their unconditional love and support which help me accomplishing my dream. Last but not least, I want to thank my brother Pankaj for always standing by side in all situations.

Synopsis

Density functional theory (DFT) has emerged as one of the most widely used tools to calculate ground state properties of materials. It has flexibility to explain the underlying physics behind various exotic materials. It can also predict the nature of unknown compounds which are hard to realize experimentally. In this work we have studied the effect of pressure on materials. Pressure has remained one of the most widely studied parameters which can drive a system towards a phase transition or induce anomaly in the electronic or vibrational properties of materials.

Recently identified topological nodal-line semimetal ZrSiS has emerged as one of materials where electronic structure is robust to small defect concentrations and provides the a platform to study relativistic particles in solid state systems. This material shows a large magnetoresistance, which has applications in device fabrications and also spintronics. We have studied the transport properties of this material by applying various pressures which is interesting to look at, as pressure can have significant effect on the properties of the topological materials. The other work in thesis is based on a widely known thermoelectric material PbTe. In this work I have tried to understand the evolution of energy bands under pressure. The strain in the system is important to understand as it helps in the designing of materials by substitution of the different atoms. We have showed the interactions among different orbitals and how they evolve under pressure.

My thesis is divided into four chapters. The first chapter describes the pressure dependent studies and why they are important and how can this be realized using density

functional theory. Then briefly I will discuss about the energy bands in solids and how one can get insight into it by looking at the density of states. Later, I have discussed about what are semimetals and their difference with the topological semimetals and briefly described what are nodal-line semimetals. The second chapter describes the methods and formalism of the density functional theory. A brief introduction of the semi-classical Boltzmann transport theory is given which was used to calculate the transport property of the ZrSiS. The third chapter describes the effect of pressure on the electronic properties of ZrSiS and the fourth chapter describes the evolution of the energy bands in PbTe under pressure.

Contents

List of Figures

List of Tables

Chapter 1

Introduction

1.1 Effect of pressure on materials

Pressure has remained one of the important parameters whose effect is widely studied to gain insight into the various types of phase transitions in solids. The phase transitions induced by pressure are important as they help in designing new materials which are of great significance to the electronic industry. It was predicted that, if sufficiently high pressure is applied to hydrogen, one can get a high-temperature superconducting state [1]. Thus, pressure is also important to understand fundamental laws which govern properties of various solids. Pressure can induce structural transition [2, 3, 4] or can affect the electronic, vibrational and transport properties of materials [5, 6, 7]. The application of pressure on any material increases the interactions and in general increases the scattering processes as the particles are confined to a smaller volume. To determine these properties, density functional theory has emerged as widely accepted method to determine the ground state properties of materials. The density functional theory can predict the properties at high pressures. The density functional theory provides a way to handle the many-body problem, which will be discussed in detail in next chapter.

In my thesis, I have studied the effect of pressure on electronic properties of nodal-line

semimetal ZrSiS and widely known thermoelectric material PbTe. First, I will discuss about topological semimetals (TSMs) and then I will introduce nodal-line semimetals (NLSMs).

1.2 Topological semimetals

After the recent advancement in the field of materials which showcase electronic structure with a non-trivial topology, a lot of efforts are put to realize new materials which have unique band topology and can provide a platform to study the underlying physics. It is expected that these materials will find applications in advanced devices. In these materials, the charge carriers show characteristics which are different from trivial semimetals or insulators [8]. After the discovery of topological insulators (TIs) [9], now the focus of scientific community has shifted to the TSMs. In ordinary metals, the properties are unique to Fermi surface, whereas normal insulators are characterized by a large gap between valence band maxima and conduction band minima.

Topological semimetal (TSM), as the term says, includes all semimetals which have some unique characteristic to their electronic structure. The *gap-less* electronic structure of semimetals is different from metals, where the charge is balanced i.e. the number density of electrons and holes in these materials is same. There are large number of topological semimetals predicted in review by Schoop et al[10].

Upon the discovery of graphene, which set an example that free-standing layered materials which have a thickness of few atoms can be realized experimentally [11]. Graphene also showed the way to realize exotic electronic properties [12]. The two doubly-degenerate linear bands which cross at a point, known as Dirac point, provided the observation of massless Dirac fermions for first time in a two-dimensional material.. In this scenario, the expression for the effective mass of electron, which depends on double derivative of $E(k)$ with respect to wave vector k, is not valid as the double derivative reduces to zero, and

hence the name massless Dirac fermions was given. Next, I will discuss about types of TSMs and difference between them.

1.2.1 Types of Topological Semimetals

There are three types of TSMs: Dirac semimetals (DSM), Weyl semimetals (WSMs) and nodal-line semimetals (NLSMs). Now, I will discuss about what are these materials and few experimental examples which are reported.

Dirac semimetals

A Dirac semimetal is characterized by two doubly degenerate linear bands which cross at a point, which is known as Dirac node. This linear band crossing occurs near the Fermi level. To find these kind of systems, both time-reversal symmetry and inversion are needed. The Dirac node, as shown in Fig. 1.1, is four-fold degenerate. Due to gapless nature of electronic structure, the electrons posses very high velocity and they are systems which provide a platform to study relativistic particles.

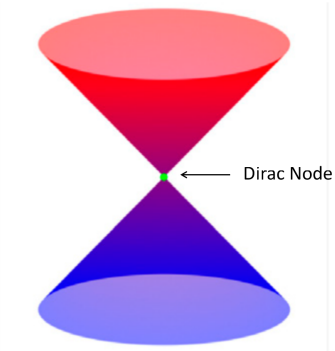

Figure 1.1: *Schematic of Dirac semimetal which shows linearly dispersed bands around the point node known as Dirac node. Both time-reversal symmetry and inversion are present. Figure courtesy of Yang et al.* [13]

There are few reports which suggested the presence of three-dimensional Dirac semimet-

als (3D DSMs). It was first confirmed in Na_3Bi [14, 15] and Cd_3As_2 [16, 17, 18].

Weyl semimetals

The Weyl semimetals are different from the Dirac semimetals in the sense that either inversion or time-reversal symmetry should be broken, which causes the separation of the two doubly degenerate bands due to spin-orbit coupling. This forces the condition where Weyl nodes can appear only in pairs with opposite chirality .

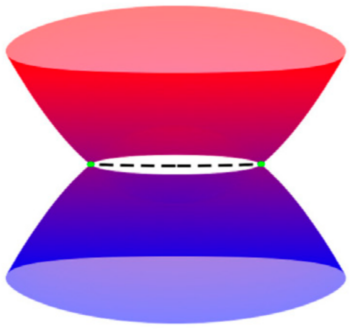

Figure 1.2: *Schematic of Weyl semimetal. The two green dots denote the weyl nodes and the dotted line which connects the two nodes. This scenario is observed when either time-reversal symmetry or inversion symmetry is broken. Figure courtesy of Yang et al.* [13]

The Weyl nodes exist near the Fermi surface. This leads to some unique features like Fermi surface arcs on the surface and chiral anomaly in the bulk [1.2]. This is discussed in the review by Yang et al. [13], with several examples where Weyl-states were observed in inversion symmetry breaking compounds like TaAs, NbAs and NbP etc [19, 20, 21]. Both Weyl and Dirac semimetals showcase zero-dimensional band crossings.

Nodal-Line semimetals

The DSMs and WSMs have zero-dimensional bands crossings. In nodal-line semimetals, there are bands crossings along which are along certain lines in the momentum space.

These lines can be in shape of a ring or a line. These systems are symmetry protected and the depending on this criteria, nodal line semimetals are of two types i.e. Dirac Nodal line semimetals and Weyl Nodal Line semimetals.

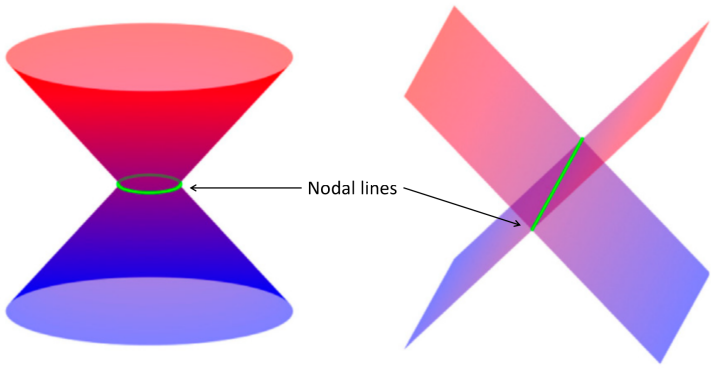

Figure 1.3: *Schematic of nodal line and nodal ring semimetal. In the momentum space the bands touch along lines forming a ring or one-dimensional line. The green circle/line denoted the band crossings. Figure courtesy of Yang et al.* [13]

The Dirac nodal line semimetals require both inversion and time-reversal symmetry to be present in the system, and under the presence of weak spin-orbit coupling the four fold degenerate line, as compared four fold degenerate point in Dirac semimetals, is formed. The Weyl nodal line semimetals have either time-reversal symmetry or inversion symmetry which causes the splitting of four fold degenerate nodal lines, and hence, two singly degenerate nodal lines are obtained. The experimentally verified nodal line semimetals are $PbTaSe_2$ [22], $PtSn_4$ [23] and ZrSiS [10, 24] and it similar analogues. In the third chapter, I have discussed about the effect of pressure on electronic transport of ZrSiS. The electronic conductivity is obtained through semi-classical Boltzmann transport theory. In ZrSiS, the nodal lines are protected by non-symmorphic symmetry [24].

1.3 Methods and Formalism

Density functional theory has become one of the major computational methods which is very helpful in the underlying physics of the condensed matter systems. It provides a method to determine the ground state properties of various systems. The importance of total energy calculations lies in the fact that many properties are first and second derivatives of the total ground state energy. Properties which are first order derivatives of total energy are forces, magnetization and polarization with respect to atomic displacement, magnetic and electric field respectively. The second order derivatives of total energy with respect to strain, magnetic and electric field gives elastic moduli, magnetic susceptibility and dielectric constant respectively. In the next section I will discuss about the fundamental aspects of the density functional theory. Later, I will discuss about semi-classical Boltzman transport equations which are used to determine the electrical conductivity and Hall coefficient.

1.4 The Density Functional Theory

The interactions between different types of particles have been remained the center of attention to the scientific community. Irrespective of the type of particles, for e.g. colloidal or subatomic particles, the interactions define the property of the material taken into consideration. The interactions between the subatomic properties are very interesting as they cannot be described by the classical laws of physics. The quantum interactions play a major role in defining properties of material. Understanding of these interactions is very important as these play important role in defining transport properties, phase transition, lattice dynamics etc. Regardless of the type of bonding, any solid can be described in terms of interactions between the electrons and the nuclei, which are coupled together. The Hamiltonian of any solid is given by,

$$\hat{H} = -\sum_i \frac{\hbar^2}{2m}\nabla_i^2 - \sum_I \frac{\hbar^2}{2M_i}\nabla_I^2 + \frac{1}{2}\frac{1}{4\pi\varepsilon_0}\sum_{i\neq j}\frac{e^2}{|r_i - r_j|} + \frac{1}{2}\frac{1}{4\pi\varepsilon_0}\sum_{i\neq j}\frac{e^2}{|R_I - R_J|} - \frac{1}{4\pi\varepsilon_0}\sum_{iI}\frac{Z_I e^2}{|r_i - R_I|} \tag{1.1}$$

where m is the mass of the electron and M_I and $Z_I e$ are the mass and charge of nucleus, i, r_i and R_I denote the positions of the ith electron and the Ith nucleus. The Hamiltonian in the Equation 1.1 can now be written in the following form, where $\hat{T}$ is the kinetic energy operator, $\hat{V_{ext}}$ is the external potential due to the background ions, $\hat{V_{int}}$ is the electron-electron interaction and E_{II} is the interaction between the nuclei,

$$\hat{H} = \hat{T} + \hat{V_{ext}} + \hat{V_{in}} + E_{II} \tag{1.2}$$

Given the total Hamiltonian we can write the time-independent Schrödinger equation as,

$$\hat{H}\Psi(\mathbf{R}, \mathbf{r}) = \epsilon\Psi(\mathbf{R}, \mathbf{r}) \tag{1.3}$$

where $\Psi(\mathbf{R}, \mathbf{r})$ is total wave function of the system. In principle all the ground state properties can be derived if we can solve the Eq.1.3. But as in real materials, there are a large number of ions and electrons. The electrons move very fast as compared to the nuclei. So, this becomes the first approximation that nuclei are at rest with respect to the nuclei where we can decouple the motion of the two. This is known as *Born-Oppenheimer* approximation or adiabatic approximation [25]. Separating the motion of the nuclei and electrons is of great help in speeding up the calculations. It should be noted that there are various kinds of interactions in a material like e^--e^- scattering or e^--phonon scattering etc, i.e. the degrees of motion of the electrons and phonons are coupled to each

other, which makes it difficullt to determine the exact form of the differential equation associated with a real system. This is where approximations like *Born-Oppenheimer* approximation and effectiveness of pseudopotentials comes into picture, which mainly are implemented to decouple the degrees of freeedom without greatly affecting the properties to be determined. The adiabatic approximation works well for semiconductors or materials with large band gaps but not for metals, superconductors or strongly-correlated systems. In these types of materials, the motion of electrons and phonons are strongly coupled and there is anharmonicity present in the system which cannot be treated under the adiabatic approximation. It is well known that the mass of nucleus much larger than that of an electron, so in general it can be assumed that the wave functions of nucleus do not overlap and one can treat the nucleus as classical particles.

1.4.1 Thomas-Fermi theory

Llewellyn Thomas and Enrico Fermi gave a quantum mechanical model which helped in understanding of electronic structure of many-body sytems comprising of large number of particles by treating them semi-classicallly, known as Thomas-Fermi model. It takes into account the electron density alone and is different from the wave function theory. It is somewhat similar to density functional theory in the sense that it make the use electronic density. This model gives an insight into form of electron density (ρ) and kinetic energy density of electrons ($t[\rho]$). It can be easily proved that for a homogeneous electron gas ρ and $t[\rho]$ have the following form,

$$\begin{aligned} \rho &= \frac{1}{3\pi^2}\left(\frac{2m\epsilon_F}{\hbar^2}\right)^{\frac{3}{2}}, \\ t[\rho] &= \frac{3}{5}\frac{\hbar^2}{2m}\left(3\pi^2\rho\right)^{\frac{2}{3}} \end{aligned} \tag{1.4}$$

where ϵ_F is the Fermi energy. Now by treating the motion of electron under classical approximation, it can be shown that,

$$T = C_{kin} \int [n(\mathbf{r}]^{\frac{5}{3}} d^3r \tag{1.5}$$

Now, the total energy of the e^- moving in a background charge can be given by,

$$H_e = C_{kin} \int [n(\mathbf{r}]^{\frac{5}{3}} d^3r + \int n(\mathbf{r}) v_{ext}(\mathbf{r}) d\mathbf{r} + \frac{1}{2} \iint \frac{\rho(\mathbf{r})\rho(\mathbf{r}')}{|\mathbf{r} - \mathbf{r}'|} d^3r d^3r' \tag{1.6}$$

where, v_{ext} is the background potential due to the nuclei and the third term represents the coulomb interaction between the electrons. Later Dirac [26] and Wigner [27] introduced the exchange and correlation effects in the electronic Hamiltonian. This we will discuss in the later section.

1.4.2 Hohenberg-Kohn theorem

The formulation of the modern density functional theory is based upon the the theorems given by Hohenberg and Kohn in 1964 [28]. They showed a way to handle many-body problem where there are interacting particles which are moving under the influence of an external potential $v_{ext}(\mathbf{r})$. The electronic Hamiltonian which is an example of interacting particles, can be written as,

$$H_e = T_e + v_{ext}(\mathbf{r}) + U_{ee}(\mathbf{r}) \tag{1.7}$$

where $U_{ee}(\mathbf{r})$ accounts for e^--e^- interaction. These theorems make use of the ground state electron density $\rho_0(\mathbf{r})$ of the system.

***First Hohenberg-Kohn Theorem*:** The external potential v_{ext} in which a system of interacting particles is moving, can be uniquely determined by the ground state electron

density $\rho_0(\mathbf{r})$.

***Second Hohenberg-Kohn Theorem*:** Associated with any external potential v_{ext}, an energy functional $E[\rho(\mathbf{r})]$ can be defined, and the ground state energy of a system is the global minimum of this energy functional.

It should be noted that the electron density $\rho(\mathbf{r})$, which minimizes $E[\rho(\mathbf{r})]$ is called the ground state density $\rho_0(\mathbf{r})$ of the system.

1.4.3 Kohn-Sham approach

The basic formulation were known till 1960s, but the main problem was to develop a scheme where one can determine the unknown total energy density functional which can be further used in the calculations. This problem was solved by Kohn and Sham [29] in 1965, by assuming a system of non-interacting particles in an external potential which was the central scheme to their approach to density functional theory. Their attempt was to find a system of non-interacting particles which could produce the same electronic density as that in a system where all particles are interacting. The unknown energy functional in the Hohenberg and Kohn theorems was simply the kinetic energy of the electrons in the Kohn-Sham approach. The main idea behind using a non-interacting system of particles is to reduce wave of a many-body system to a single particle wave-function. The kinetic energy calculated using this approximation is not accurate as it is not same as the kinetic energy derived from a many-body wave function. So, the use of single particle wave-function remainsthe prime idea behind the Kohn-Sham approach.

Now, since energy density functional make use of the electron density, in terms single particle wave-function the electron density can be written as,

$$\rho(\mathbf{r}, \mathbf{r}') = \sum_i f_i \phi_i(\mathbf{r}) \phi^*(\mathbf{r}') \tag{1.8}$$

where $\phi_i(\mathbf{r})$ are the one electron orbitals and f_i are the occupation numbers of these single particle wave-functions. Similarily, the kinetic energy of the independent non-interacting system of the particles can written in the following form,

$$T_e = -\frac{\hbar^2}{2m}\sum_i \left\langle \phi_i(\mathbf{r})|\nabla^2|\phi^*(\mathbf{r}')\right\rangle \tag{1.9}$$

Using the Kohn-Sham approach the energy functional can now be written as,

$$E_{KS}[\rho(\mathbf{r})] = T[\rho(\mathbf{r})] + \int \rho(\mathbf{r})v_{ext}(\mathbf{r})d\mathbf{r} + \frac{1}{2}\iint \frac{\rho(\mathbf{r})\rho(\mathbf{r}')}{|\mathbf{r}-\mathbf{r}'|}| + E_{xc}[\rho(\mathbf{r})] \tag{1.10}$$

The first term is the kinetic energy of the system of non-interacting particles which in are moving in an external potential $v_{ext}(\mathbf{r})$. The second term takes into account the effect of background potential on e^-s. The third term is the coulomb interaction of the electrons among themselves. The fourth term accounts for the *exchange-correlation* interaction between the electrons. The Eq. 1.10 can be represented in a more compact form similar to Schrödinger equation as,

$$\left(-\frac{\hbar^2}{2m}\nabla_I^2 + V_{KS}(\mathbf{r})\right)\Psi_i(\mathbf{r}) = \varepsilon_i\Psi_i(\mathbf{r}) \tag{1.11}$$

where V_{KS} is the Kohn-Sham potential for the non-interacting system given as,

$$V_{KS}(\mathbf{r}) = v_{ext}(\mathbf{r}) + \int \frac{n(\mathbf{r}')}{|\mathbf{r}-\mathbf{r}'|}d\mathbf{r} + V_{xc}[\rho(\mathbf{r})] \tag{1.12}$$

where v_{ext} is the external potential due to background charge, electric or magnetic field,

the second term is the Hartree potential. The last term is the *exchange-correlation* potential defined as,

$$V_{xc}[\rho(\mathbf{r})] = \frac{\delta E_{xc}[\rho(\mathbf{r})]}{\delta \rho(\mathbf{r})} \tag{1.13}$$

The Eq. 1.10 needs to be minimised with respect to electronic density ρ with a constraint that the electron density upon integrating gives the total number of the electrons in the system. This minimum energy obtained is called the ground state electronic energy and the electron density which leads to it, is called the ground state electronic density $\rho_0(\mathbf{r})$. The Eq. 1.12 should be solved self-consistently making sure that the electron density used to construct V_{KS} matches to the one obtained from solving Kohn-Sham Hamiltonian (Eq.1.11).

1.4.4 Approximation to exchange and correlation interaction

The biggest challenge in density functional theory is to correctly treat the exchange-correlation functional. The most popular ones which are widely used are local density approximation (LDA) and generalizes gradient approximation.

Local-density approximations (LDA) take into account the local value of electron density or in other words depend upon the value of $\rho(\mathbf{r})$ at each point in space. Here the real inhomogeneous system is treated as locally homogeneous system. This approach is very well known for the homogeneous electron gas [30]. The exchane-correlation energy can be determined by simply integrating the exchange-correlation energy density at each point in space. Thus the exchange-correlation energy in LDA is,

$$E_{xc}^{LDA}[\rho] = \int \rho(\mathbf{r}) \epsilon_{xc}[\rho] d^3\mathbf{r} \tag{1.14}$$

The local density approximation works well for systems where the electron density is quite uniform like metallic systems where the free electron model is a fair approximation. The main drawback of this type of interaction that it fails to estimate band gap of the materials like semiconductors or materials where there is a large correlation between the electrons and phonons or any other quasiparticle. For a free electron gas the energy level are continuous or in other words the excitations are gap-less. LDA is also not suitable for determining the weak inter-molecular bonds, hydrogen bonds etc.

A better approximation that LDA was generalised gradient approximation (GGA). This included various aspectswhich were completely ignored in the LDA approximation. This approximation treats the electrons in a inhomogeneous way. In this way one can upto some extent take into account the correlations of electrons in a more exact way. This is the reason why GGA works better in the case of semiconductors or correlated systems. The exchange-correlation energy in GGA is,

$$E_{xc}^{GGA}[\rho] = \int \rho(\mathbf{r})\epsilon_{xc}[\rho()\mathbf{r}, |\nabla\rho|, |\nabla^2\rho|]d^3\mathbf{r} \tag{1.15}$$

In GGA there is presence of non-local exchange correlation effect. These potentials are generally used to determine electron-phonon coupling constants. These potentials are more accurate than LDA. We have used GGA approximation in all the work presented in this thesis.

1.5 Pseudopotentials

In most of the software packages which provide an efficient way of obtaining the electronic and vibrational properties of the material, through density functional calculations make use of the pseudopotentials. Here, we will discuss about the widely used pseudopotentials

method. It can be observed that the band structure we obtained 2.5 is quite similar to the one calculated by Schoop et al. [31], where they made the use of *all-electron* potentials. We will discuss about the reasons why pseudopotential are more easy to use than all-electron potentials.

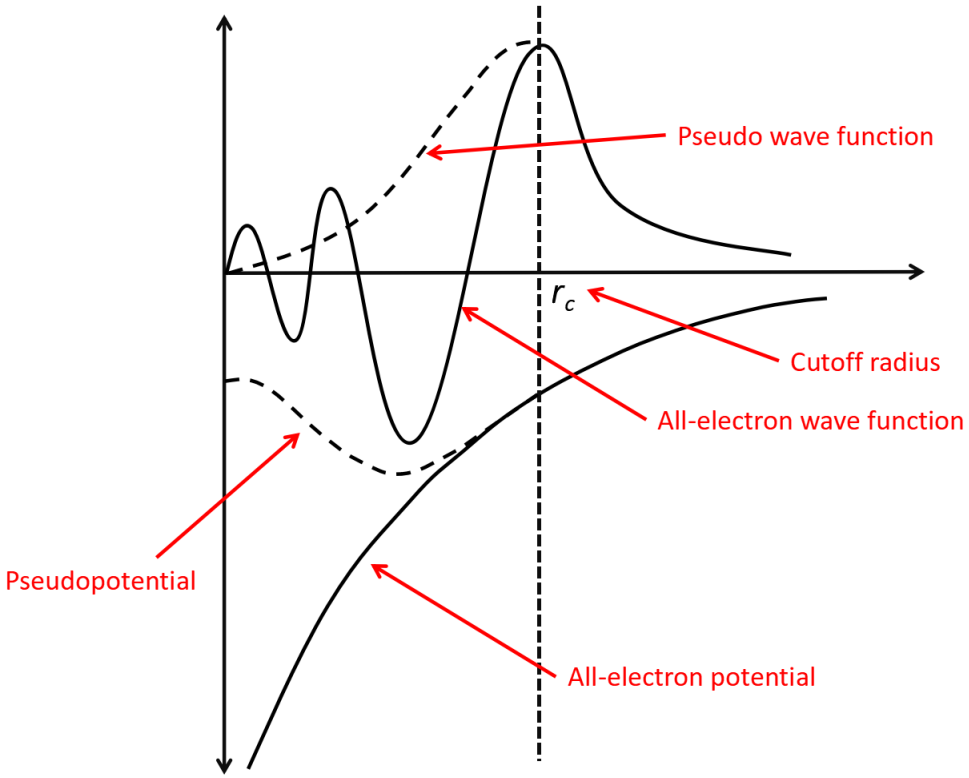

Figure 1.4: *Above plot shows the difference between all-electron potential and pseudopotential. Here, r_c is the cutoff radius above which both type of potentials and wavefunctions overlap. (https://en.wikipedia.org/wiki/Pseudopotential)*

To give basic idea about psudopotentials, consider the electronic configuration of Si atom is $1s^2 2s^2 2p^6 3s^2 3p^2$. It is well known that properties of a material are determined by the valence electrons. In solids, there is overlap of the atomic wave-functions. So, it can be easily understood that valence electrons contribute to the overlap of the orbitals. The inner $1s$, $2s$ and $2p$ orbitals form the core of the atoms and do not take part in the bonding, whereas the outer $3s$ ans $3p$ orbitals are partially filled and form bonds with other atoms

through wave function overlap. In crystalline Si, which has diamond structure, each Si atom is bonded to its four nearest neighbours through sp^3 hybridized orbitals. So, it can be understood that these valence electrons do not feel the full force of the nuclei and are nearly free. The wave functions of electron in the core region should be orthogonal to that of the core electrons. So, the wave functions near the core have strong oscillatory nature which make it difficult to solve the wave equation. To overcome this difficulty, the true wave function is divided into two parts i.e. a smooth part (**pseudo-wave function**) and an oscillatory part. In this way, the strong true potential is replaced by a weaker effective potential or **pseudopotential** for the valence electrons, which are not much affected by the shape of wave function near the core [32]. The basic requirement for a pseudopotential is,

$$\begin{aligned} V_{pseudo} &= V_{ae} \quad r \geq r_c \\ \psi_{pseudo} &= \psi_{ae} \quad r \geq r_c \end{aligned} \tag{1.16}$$

From Fig.1.4, it can be observed that a cutoff radius must be defined to treat the valence electrons in same manner as that in an all-electron potential, and also it shows that all-electron potential is oscillatory near the core and smooth after the cutoff radius. The cutoff radius depends on the size of the atom and the number of outer shells one wants to include in the calculations. This shows that only by treating the valence electrons one can still find the various properties like lattice constant, bulk modulus, elastic constants etc. There are many developed pseudopotential libraries which are readily available. In the next section we will discuss about the semi-classical Boltzmann tranport theory which was used to calculate transport properties.

1.6 Semi-Classical Boltzmann transport theory

The *Boltzmann equation* or *Boltzmann transport equation* is widely used to determine the transport properties of the particles in solid, liquid or gas. It aims at non-equilibrium systems and is often focused on determining the transport properties of charge, heat or mass etc., which are further related to electrical conductivity, thermal conductivity or mass conductivity etc., respectively. It is also the basis of semi-classical theories of transport equation i.e. the motion of quantum particles (i.e. electrons) will be determined by using the laws which are similar to the Newton's equation of the motion [33]. Here, we will discuss about the underlying equation which determine the electrical conductivity. The out of equilibrium population of electrons is given by,

$$f = \frac{1}{1 + e^{\frac{E - E_F}{kT}}} \tag{1.17}$$

Now, consider electron moving under electric field. The equation of motion can be written as,

$$\frac{d(\hbar \mathbf{k})}{dt} = -\nabla \mathbf{E}(\mathbf{r}) \tag{1.18}$$

It can be also be shown that group velocity v_g of the electrons can be written as,

$$v_g(t) = \frac{1}{\hbar} \nabla_k E(k) \tag{1.19}$$

The group velocity of the electrons in a electronic band is also related to the effective mass. If particles have higher group velocity, the effective mass will be lower. Let the probability of a particle moving along x-direction in phase space is $f(x, p_x, t)$. After Δt

time, the probability of the particle is $f(x - v_g dt, p - F_e dt, t - dt)$. For a slowly varying energy level,

$$\begin{aligned} f(x, p_x, t) &= f(x, p_x, t) \\ \frac{df}{dt} &= 0 \end{aligned} \tag{1.20}$$

This is collisionless *Boltzmann transport equation*, where the transport of the electrons is ballistic. In deriving the above expression the scattering time is not taken into account. There are various scattering processes like electron-electron scattering, electron-phonon scattering and scattering from defects, vacancies or other impurities etc. In the presence of these interactions, the momenta of electrons is not conserved and hence the distribution function $f(r, p, t)$ is no longer conserved, which means that $\mathrm{d}f/\mathrm{d}t \neq 0$. So, there is a need of introduction of scattering processes into the transport equation. This is done by incorporating the collision integral $C[f]$, which is a functional of the distribution function. The transport equation can be written as,

$$\frac{df(\mathbf{r}, \mathbf{p}, t)}{dt} = C[f] \tag{1.21}$$

Apart from scattering processes, in semiconductors there is generation and recombination processes of electrons and holes are also present. For certain temperature ranges there can be difference in the rate of generation and recombination of the electrons and holes, which affects the population of the charge carriers. In simple terms, the collision integral can be written as,

$$C[f] = \sum_{\mathbf{p}'} (\mathbf{W}_{\mathbf{p}'-\mathbf{p}} - \mathbf{W}_{\mathbf{p}-\mathbf{p}'}) \tag{1.22}$$

where $\mathbf{W_{p'-p}}$ is the probabilty per unit time that an electron will undergo scattering process and during this its momenta changes from $\mathbf{p'}$ to $\mathbf{p}$. Defining the collision integral in this way incorporates the microscopic probabilities associated with quantum transitions. For most of the cases the equations are solved for the case where the *relaxation time* τ is direction independent. Due to this approximation, Seebeck and Hall coefficients are independent of τ. The expression for electrical conductivity and the Hall coefficient implemented in the Boltztrap code [34], which works under these approximations are,

$$\sigma_{\alpha\beta}(T;\mu) = \frac{1}{\Omega}\int \sigma_{\alpha\beta}(\varepsilon)\Big[-\frac{\partial f_{\mu}(T;\varepsilon)}{\partial\varepsilon}\Big]d\varepsilon \tag{1.23}$$

$$R_{ijk} = \frac{E_j^{ind}}{j_i^{appl}B_k^{appl}} \tag{1.24}$$

where $\sigma_{\alpha\beta}(\varepsilon)$ is given by,

$$\sigma_{\alpha\beta}(\varepsilon) = \frac{e^2}{N}\sum_{i,\mathbf{k}} \tau v_{\alpha}(i,\mathbf{k})v_{\beta}(i,\mathbf{k})\delta(\varepsilon-\varepsilon_{i,\mathbf{k}}) \tag{1.25}$$

where $\mathbf{k}$ and i are wave vectors and band index. In Eq.1.25, N denotes the total number of the k-points used to sample the Brillouin zone. In general, the number of k-points used for calculations should be very large to obtain reasonable values of the transport coefficients. Here, α and β denote the cartesian coordinates and, v_{α} is the group velocity given by,

$$v_{\alpha} = \frac{1}{\hbar}\frac{\partial\varepsilon_{i,\mathbf{k}}}{\partial k_{\alpha}} \tag{1.26}$$

Above equations are implemented in the Bolztrap code. All our calculations are done under these approximations. In chapter 3, we have showed calculated results of temperature dependent electrical conductivity and Hall coefficient. The electrical conductivity obtained is normalised with respect to relaxation time.

Bibliography

[1] N. W. Ashcroft, "Metallic hydrogen: A high-temperature superconductor?," *Physical Review Letters*, vol. 21, no. 26, p. 1748, 1968.

[2] J. Z. Hu, L. D. Merkle, C. S. Menoni, and I. L. Spain, "Crystal data for high-pressure phases of Silicon," *Phys. Rev. B*, vol. 34, pp. 4679–4684, Oct 1986.

[3] T. Ishidate, S. Abe, H. Takahashi, and N. Môri, "Phase diagram of $BaTiO_3$," *Phys. Rev. Lett.*, vol. 78, pp. 2397–2400, Mar 1997.

[4] J. Besson, J. Itie, A. Polian, G. Weill, J. Mansot, and J. Gonzalez, "High-pressure phase transition and phase diagram of gallium arsenide," *Physical Review B*, vol. 44, no. 9, p. 4214, 1991.

[5] H. Suderow, V. Tissen, J. Brison, J. Martínez, and S. Vieira, "Pressure induced effects on the Fermi surface of superconducting 2H-$NbSe_2$," *Physical review letters*, vol. 95, no. 11, p. 117006, 2005.

[6] W. Paul and G. L. Pearson, "Pressure dependence of the resistivity of Silicon," *Phys. Rev.*, vol. 98, pp. 1755–1757, Jun 1955.

[7] M. Leroux, I. Errea, M. Le Tacon, S.-M. Souliou, G. Garbarino, L. Cario, A. Bosak, F. Mauri, M. Calandra, and P. Rodière, "Strong anharmonicity induces quantum melting of charge density wave in 2H-$NbSe_2$ under pressure," *Physical Review B*, vol. 92, no. 14, p. 140303, 2015.

[8] J. Xiong, S. K. Kushwaha, T. Liang, J. W. Krizan, M. Hirschberger, W. Wang, R. Cava, and N. Ong, "Evidence for the chiral anomaly in the Dirac semimetal Na_3Bi," *Science*, vol. 350, no. 6259, pp. 413–416, 2015.

[9] M. Z. Hasan and C. L. Kane, "Colloquium: Topological insulators," *Rev. Mod. Phys.*, vol. 82, pp. 3045–3067, Nov 2010.

[10] L. M. Schoop, F. Pielnhofer, and B. V. Lotsch, "Chemical principles of topological semimetals," *Chemistry of Materials*, vol. 30, no. 10, pp. 3155–3176, 2018.

[11] A. K. Geim and K. S. Novoselov, "The rise of graphene," in *Nanoscience and Technology: A Collection of Reviews from Nature Journals*, pp. 11–19, World Scientific, 2010.

[12] K. S. Novoselov, A. K. Geim, S. Morozov, D. Jiang, M. Katsnelson, I. Grigorieva, S. Dubonos, and A. Firsov, "Two-dimensional gas of massless Dirac fermions in graphene," *nature*, vol. 438, no. 7065, p. 197, 2005.

[13] S.-Y. Yang, H. Yang, E. Derunova, S. S. Parkin, B. Yan, and M. N. Ali, "Symmetry demanded topological nodal-line materials," *Advances in Physics: X*, vol. 3, no. 1, p. 1414631, 2018.

[14] Z. Wang, Y. Sun, X.-Q. Chen, C. Franchini, G. Xu, H. Weng, X. Dai, and Z. Fang, "Dirac semimetal and topological phase transitions in a 3 bi (a= na, k, rb)," *Physical Review B*, vol. 85, no. 19, p. 195320, 2012.

[15] Z. Liu, "Zk liu, b. zhou, y. zhang, zj wang, hm weng, d. prabhakaran, s.-k. mo, zx shen, z. fang, x. dai, z. hussain, and yl chen, science 343, 864 (2014).," *Science*, vol. 343, p. 864, 2014.

[16] M. Neupane and S.-Y. Xu, "M. neupane, s.-y. xu, r. sankar, n. alidoust, g. bian, c. liu, i. belopolski, t.-r. chang, h.-t. jeng, h. lin, a. bansil, f. chou, and mz hasan, nat. commun. 5, 3786 (2014).," *Nat. Commun.*, vol. 5, p. 3786, 2014.

[17] Z. Liu, J. Jiang, B. Zhou, Z. Wang, Y. Zhang, H. Weng, D. Prabhakaran, S. Mo, H. Peng, P. Dudin, *et al.*, "A stable three-dimensional topological Dirac semimetal Cd_3As_2," *Nature materials*, vol. 13, no. 7, p. 677, 2014.

[18] S. Borisenko, Q. Gibson, D. Evtushinsky, V. Zabolotnyy, B. Büchner, and R. J. Cava, "Experimental realization of a three-dimensional Dirac semimetal," *Physical review letters*, vol. 113, no. 2, p. 027603, 2014.

[19] S.-Y. Xu, I. Belopolski, N. Alidoust, M. Neupane, G. Bian, C. Zhang, R. Sankar, G. Chang, Z. Yuan, C.-C. Lee, *et al.*, "Discovery of a Weyl fermion semimetal and topological Fermi arcs," *Science*, vol. 349, no. 6248, pp. 613–617, 2015.

[20] S.-Y. Xu, N. Alidoust, I. Belopolski, Z. Yuan, G. Bian, T.-R. Chang, H. Zheng, V. N. Strocov, D. S. Sanchez, G. Chang, *et al.*, "Discovery of a Weyl fermion state with Fermi arcs in niobium arsenide," *Nature Physics*, vol. 11, no. 9, p. 748, 2015.

[21] S. Souma, Z. Wang, H. Kotaka, T. Sato, K. Nakayama, Y. Tanaka, H. Kimizuka, T. Takahashi, K. Yamauchi, T. Oguchi, *et al.*, "Direct observation of nonequivalent Fermi-arc states of opposite surfaces in the noncentrosymmetric Weyl semimetal NbP," *Physical Review B*, vol. 93, no. 16, p. 161112, 2016.

[22] G. Bian, T.-R. Chang, R. Sankar, S.-Y. Xu, H. Zheng, T. Neupert, C.-K. Chiu, S.-M. Huang, G. Chang, I. Belopolski, *et al.*, "Topological nodal-line fermions in spin-orbit metal $PbTaSe_2$," *Nature communications*, vol. 7, p. 10556, 2016.

[23] Y. Wu, L.-L. Wang, E. Mun, D. D. Johnson, D. Mou, L. Huang, Y. Lee, S. L. Bud'ko, P. C. Canfield, and A. Kaminski, "Dirac node arcs in $PtSn_4$," *Nature Physics*, vol. 12, no. 7, p. 667, 2016.

[24] L. M. Schoop, M. N. Ali, C. Straßer, A. Topp, A. Varykhalov, D. Marchenko, V. Duppel, S. S. Parkin, B. V. Lotsch, and C. R. Ast, "Dirac cone protected by non-symmorphic symmetry and three-dimensional dirac line node in zrsis," *Nature communications*, vol. 7, p. 11696, 2016.

[25] M. Born and R. Oppenheimer, "Zur quantentheorie der molekeln," *Annalen der physik*, vol. 389, no. 20, pp. 457–484, 1927.

[26] P. A. Dirac, "Note on exchange phenomena in the thomas atom," in *Mathematical Proceedings of the Cambridge Philosophical Society*, vol. 26, pp. 376–385, Cambridge University Press, 1930.

[27] E. Wigner, "Effects of the electron interaction on the energy levels of electrons in metals," *Transactions of the Faraday Society*, vol. 34, pp. 678–685, 1938.

[28] P. Hohenberg and W. Kohn, "Inhomogeneous electron gas," *Physical review*, vol. 136, no. 3B, p. B864, 1964.

[29] W. Kohn and L. J. Sham, "Self-consistent equations including exchange and correlation effects," *Phys. Rev.*, vol. 140, pp. A1133–A1138, Nov 1965.

[30] P. A. Dirac, "Note on exchange phenomena in the thomas atom," in *Mathematical Proceedings of the Cambridge Philosophical Society*, vol. 26, pp. 376–385, Cambridge University Press, 1930.

[31] L. M. Schoop, M. N. Ali, C. Straßer, A. Topp, A. Varykhalov, D. Marchenko, V. Duppel, S. S. Parkin, B. V. Lotsch, and C. R. Ast, "Dirac cone protected by non-symmorphic symmetry and three-dimensional dirac line node in zrsis," *Nature communications*, vol. 7, p. 11696, 2016.

[32] Y. Peter and M. Cardona, *Fundamentals of semiconductors: physics and materials properties*. Springer Science & Business Media, 2010.

[33] F. Han, *A modern course in the quantum theory of solids*. World Scientific, 2013.

[34] G. K. Madsen and D. J. Singh, "Boltztrap. a code for calculating band-structure dependent quantities," *Computer Physics Communications*, vol. 175, no. 1, pp. 67–71, 2006.

[35] R. M. Martin, *Electronic structure: basic theory and practical methods*. Cambridge university press, 2004.

Chapter 2

Pressure induced jump in resistivity in topological nodal-line semimetal ZrSiS

2.1 Introduction

Topological semimetals provide a platform where the underlying fundamental physical phenomena of relativistic particles can be explored. These particles showing unique properties offer a great possibility of technological applications. These materials find applications in various fields of electronics due to their novel transport properties. To find these exotic states of materials, there was a lot of effort to look for robust systems which show large range of linearly dispersed bands. It was desirable that small concentrations of impurity or defects should not affect the nontrivial band topology of the materials. Discovery of Topological Insulators (TIs) [1] and Weyl semimetals [2, 3] provided the platform to study relativistic fermions and to explore their practical applications. The unique electronic structure of these materials was considered as one of the major breakthroughs in recent times.

The advancement in the computational methods to determine electronic properties led to an enormous contribution to condensed matter physics. This helped the scientific community to understand the underlying physics behind these type of materials. The theoretical methods also paved the way in design of new topological phases of matter. Since the discovery of graphene, there were many efforts to find massless fermions in the bulk. In the electronic structure of graphene, electronic bands are linear in k-space where general expression of effective mass breaks down. In this work, we have tried to understand the transport properties of nodal-line semimetal ZrSiS at various pressures. In this class of material the bands cross along a one-dimensional line instead of discrete points. This material is interesting because it shows several linear-band crossings near the Fermi level in the range 0-2 eV [4]. However, the spin-orbit coupling introduces a small gap of 20 meV. It paves the way for different interesting properties and phenomena. As shown earlier by Singha et. al, this material shows large magnetoresistance. So, it is interesting to study the behaviour of electronic transport under pressure. Pressure can have unique consequences, like the phase transition, or anomaly in scattering processes. In this work, our aim is to understand the effect of a pressure-induced jump in the resistivity at low temperature in nodal line semimetal ZrSiS. In the next section I have discussed about the experimental results, which was the main motivation behind this work.

2.2 Experimental results

Pressure causes a change in the electronic properties of materials and in general affects the scattering processes such as e^--e^- scattering or e^--phonon scattering. Most of the topological materials are quite sensitive to the application of pressure because in most cases the nontrivial topology of the electronic structure is protected by the symmetries of the system. The scattering processes in the material are also affected by the changes in the lattice parameter and determine the transport properties of electrons and other

quasiparticles. It is an important parameter which is capable of driving the system towards a structural or topological transition. This work was motivated by the pressure-dependent resistivity measurements on nodal-line semimetal ZrSiS, where an anomaly in the low-temperature resistivity was observed under pressure.

2.2.1 Crystal structure and lattice parameters

Earlier studies have reported that the structure of ZrSiS is layered and resembles PbFCl-type structure and crystallizes in tetragonal *P4/nmm* space group [5, 6], where Si-atoms in the *ab*-plane form a square mesh and Zr ans S atoms are sandwiched between the between this mesh of Si-atoms. There is weak covalent interaction between the layers and the layers cannot be exfoliated [7].

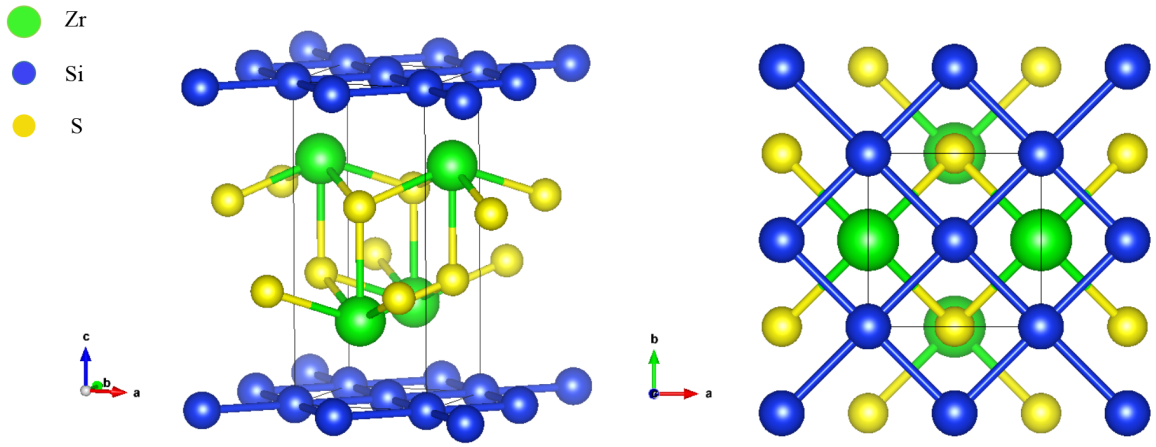

Figure 2.1: *Structure of ZrSiS (Space group: P4/nmm. There is weak covalent interaction between the layers, so exfoliation is not possible. Crystal can be compressed easily along c-axis.*

In earlier work, Singha et al. showed the presence of an orthorhombic phase coexisting with tetragonal phase above 3.7 GPa, and above 18.7 GPa, the tetragonal phase coexists with both monoclinic and orthorhombic phases [8]. The refinement of lattice parameters

was done without considering the refinement for atomic positions and it was assumed that orthorhombic phase crystallizes in the $BaBr_2$-type structure (Space group: *Pnma*) with lattice parameters of $a = 4.235$ Å, $b = 4.987$ Å and $c = 8.313$ Å at 3.7 GPa. The accurate atomic positions for the orthorhombic phase are not known.

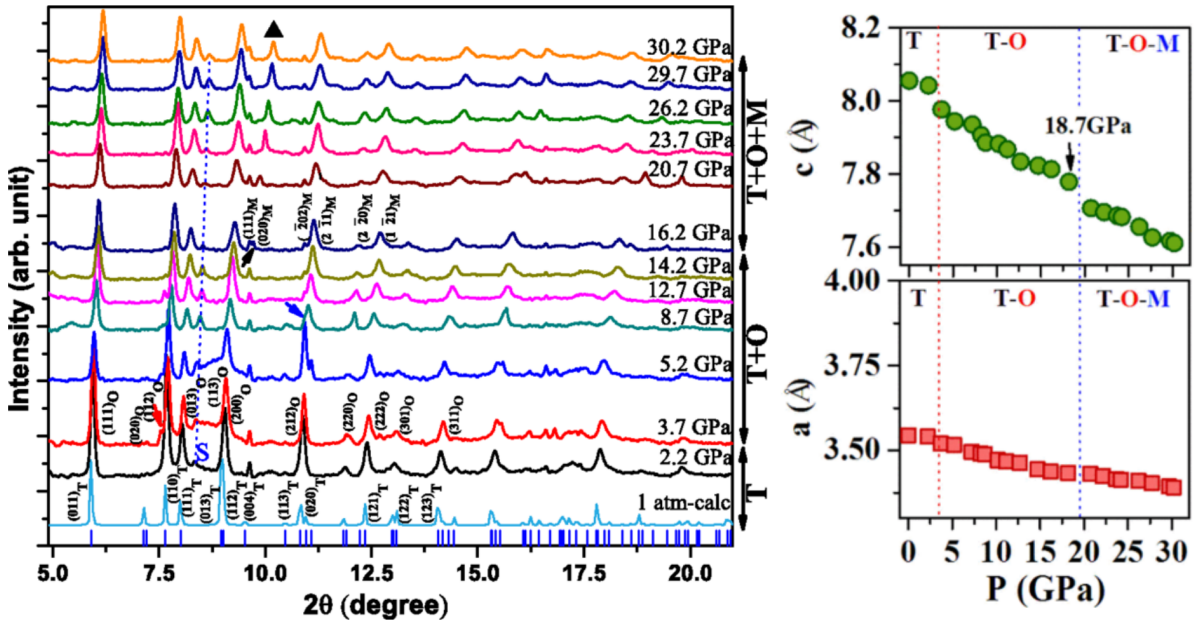

Figure 2.2: *Plots showing the pressure-dependent x-ray scattering data and the variation of the a- and c-lattice parameter. It was shown that above* 3.7 *GPa tetragonal and orthorhombic phase coexist, and above* 18.7 *GPa the parent tetragonal phase coexists with orthorhombic and monoclinic phases. Figure courtesy of Singha et al. Ref.* [8]

In this thesis, I have studied the effect of pressure on the tetragonal phase. Later, I will discuss its electronic structure and transport properties.

2.2.2 Pressure-dependent resistivity vs temperature

Earlier experimental results showed that resistivity (ρ) of ZrSiS has a metallic character and ρ continuously decreases with decrease in the temperature [9].

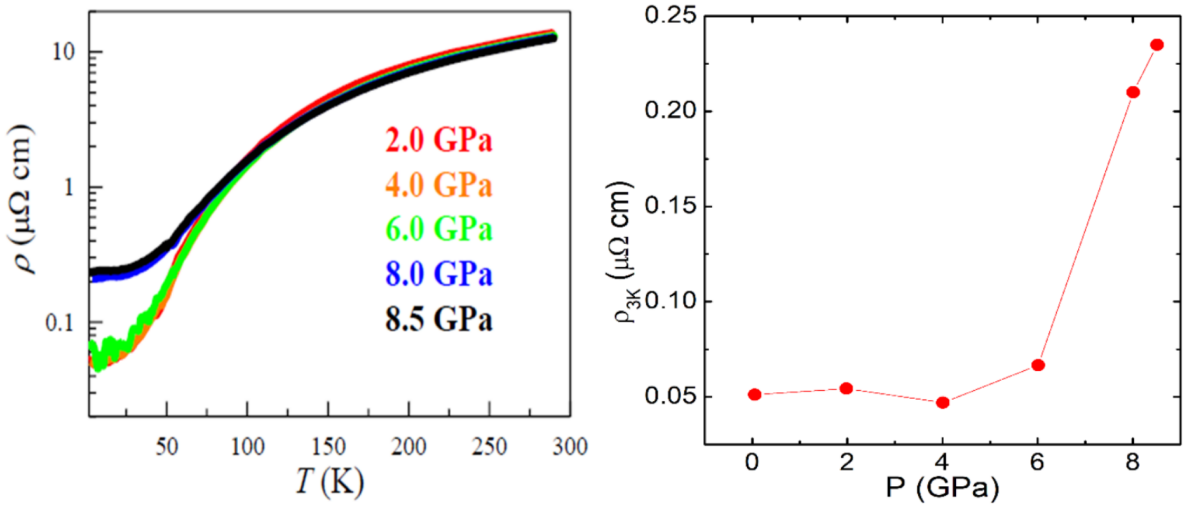

Figure 2.3: *Plots indicate the jump in the resistivity at* 6 *GPa. It can be observed that at temperatures above* 60 *K the resistivity is nearly same for all the pressures.*

Our work is motivated by experimental results (**Experiments were performed by Prof. Prabhat Mandal and his group** [1]) which show that as the pressure increases there is a jump in the low-temperature resistivity, whereas at higher temperatures there is no significant effect of pressure. It was observed that jump in the resistivity occurs above 6 GPa and results in a metal to non-metal like transition at low temperature. It can also be observed that above 60 K, the nature of the resistivity remains same at all reported pressures without major difference in the values of resistivity at various pressures. The anomaly in the resistivity is only observed at low temperatures which indicates that temperature plays a major role in determining the phase transition and transport properties.

2.3 Computational details

In this work we have tried to understand the low-temperature resistivity using first-principles density functional theory (DFT) calculations as implemented in QUANTUM

[1]Saha Institute of Nuclear Physics, 1/AF Bidhannagar, Kolkata 700064, India

ESPRESSO [10] software package. Here, the potentials used are used are ultrasoft pseudopotentials [11]. The exchange-correlation energy of electrons was treated under generalized gradient approximation (GGA) [12] and the functional form was used as parameterized by Perdew−Burke−Ernzherof [13]. The energy cutoff of wave functions in plane-wave basis set used was 50 Ry and charge density in the planewave basis set was truncated with energy cutoff of 400 Ry. A uniform $k-$point mesh of $24 \times 24 \times 16$ was used for integrations in Brillouin zone with Fermi-Dirac smearing-width of 0.003 Ry. The transport properties were calculated using BoltzTraP code [14] using a very dense k-point mesh which is implemented under a constant scattering time approximation.

2.4 Results and Discussion

Here, first we have estimated the lattice parameters.

Pressure (GPa)	**a (Å)**	**c (Å)**	**c/a**	**Volume (Å^3)**
0	3.555	8.148	2.292	103.019
1	3.546	8.128	2.292	102.235
2	3.538	8.108	2.291	101.495
3	3.530	8.081	2.288	100.751
4	3.523	8.059	2.287	100.052
5	3.516	8.038	2.286	99.378
6	3.509	8.017	2.284	98.727
7	3.502	7.997	2.283	98.098
8	3.495	7.978	2.282	97.489
9	3.489	7.960	2.281	96.900
10	3.482	7.941	2.280	96.329

Table 2.1: *Estimated lattice parameters, c/a ratio and volume of the tetragonal phase of ZrSiS at various pressures.*

The calculated lattice parameters often don't match with the experimentally deter-

mined parameters due to the implementation of generalized-gradient approximation and taking into account only the valence electrons in pseudopotentials. A minimum requirement where the results can be trusted, is that estimated lattice parameters in general should not differ from the experimentally determined parameters by more than 2%.

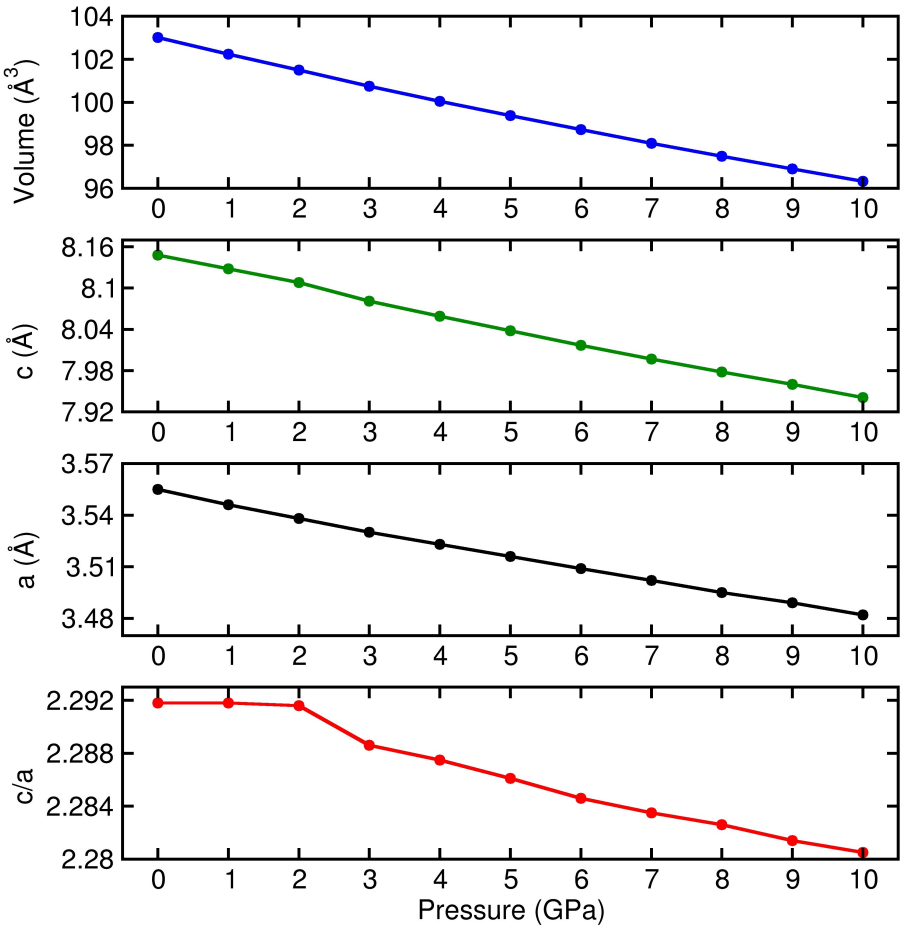

Figure 2.4: *Plots showing the variation of volume, lattice parameters and c/a-ratio. It can be observed that volume, a and c-lattice parameter decrease linearly with increase in hydrostatic pressure. c/a ratio remains nearly constant upto 2 GPa and then starts decreasing.*

It can be observed that volume, a and c-lattice parameter decrease linearly with increase in pressure. The c/a-ratio remains nearly constant upto 2 GPa, then starts decreasing linearly as the pressure decreases.

2.4.1 Electronic structure

The electronic structure of topological materials are sensitive to change in their lattice parameters and the symmetries of the crystal structure, which can be tuned by applying pressure. Pressure can drive the system towards a structural phase transition and in some cases a topological transition [15]. Here, in this work first we investigated the pressure dependence of the electronic structure of the tetragonal phase. The electrical transport of a material depends on the electrons near the Fermi level. If there is a change in the electronic structure near the Fermi level it will affect the transport properties of the material.

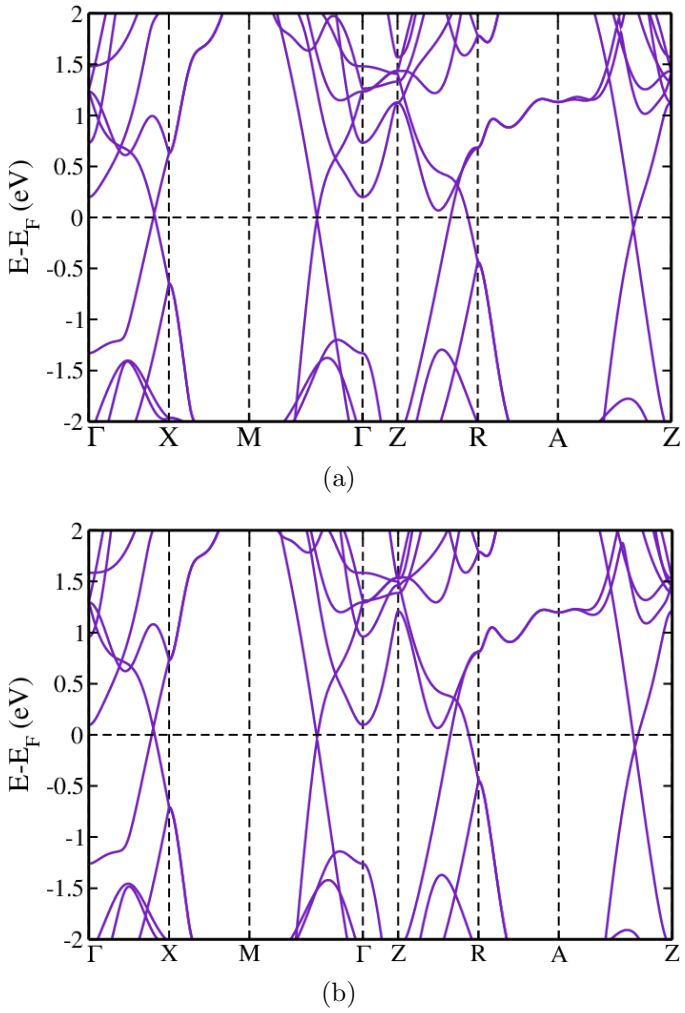

Figure 2.5: *Electronic structure of ZrSiS (Space group: P4/nmm) at (a)* 0 *GPa and (b)* 10 *GPa. The parabolic band at* Γ*-point comes closer to the Fermi level at 10 GPa.*

In the case of ZrSiS, there are multiple Dirac crossings near the Fermi level in the range of 0-2 eV and the Dirac crossings closest to the Fermi level are between ΓX- , MΓ- and AZ-paths in the brillouin zone. This material is one of the many examples of systems where massless fermions can be found in the bulk. Figure 2.5 showcases the the band structure of the tetragonal phase of ZrSiS, along high-symmetry path in brillouin zone at 0 and 10 GPa. Earlier it was also shown that cones at X and R point are not influenced by spin-orbit coupling [4]. From the band structure at 10 GPa, it can be observed that there is no significant change in the electronic structure near the Fermi level which could indicate towards the anomaly in low-temperature resistivity. At 10 GPa, it can be observed that parabolic bands at Γ-point came closer to the Fermi level. This suggests that there is a possibility of increase in conductivity due to the tetragonal phase.

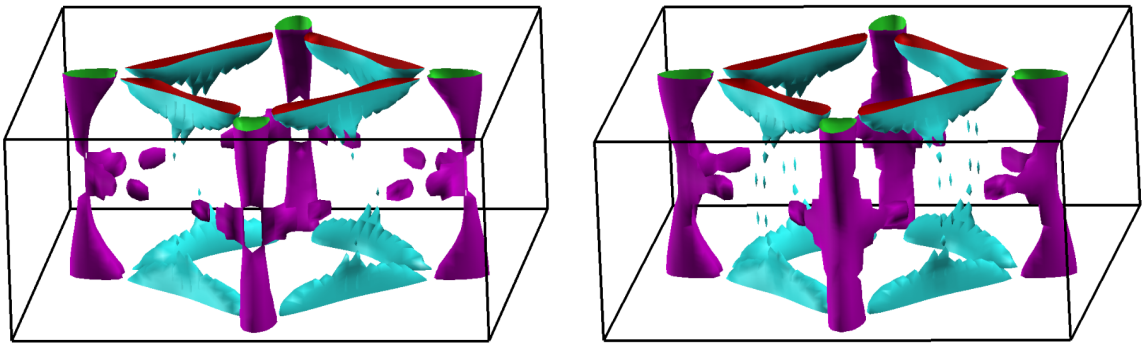

(a) (b)

Figure 2.6: *Canted view of merged band Fermi surface of ZrSiS at (a) 0 GPa and (b) 10 GPa. The Fermi surface shows tubular nature.*

In Fig. 2.6, the calculated Fermi surface is shown. At 0 GPa, a hole pocket can be observed (violet colored), which fills up at 10 GPa. This is because, the rise in pressure causes more electronic states to contribute to the Fermi surface. This also indicates an

increase in the electronic conductivity of tetragonal phase at 10 GPa.

2.4.2 Density of states

In this section, we will describe the effect of pressure observed on the density of states (DOS) of ZrSiS. This helps in understanding the changes in electronic structure from a different point of view.

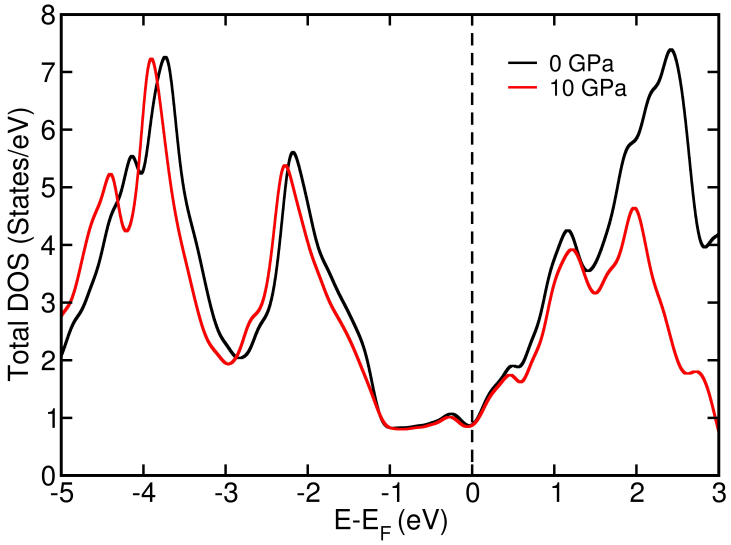

Figure 2.7: *Total density of states of ZrSiS tetragonal phase at 0 and 10 GPa. There is a shift in the corresponding peaks. Minima at Fermi level indicates the presence of pseudogap.*

In Fig.2.7, we can observed that density of states (DOS) at 10 GPa is lower than that of 0 GPa near -1 eV and above 0.5 eV. It can also be observed that DOS near Fermi level is nearly same for both pressures. It is known that the transport properties are determined by the electrons near the Fermi level. There is no significant change in the number of states at Fermi level. Also above 2eV, there is a significant decrease in the DOS at 10 GPa. A minima at Fermi level can also be observed, which indicates the presence of a pseudogap. A pseudogap occurs when certain points in brillouin zone are gapped but there are some points which are gapless. Next, we will discuss the contribution of different orbitals to DOS.

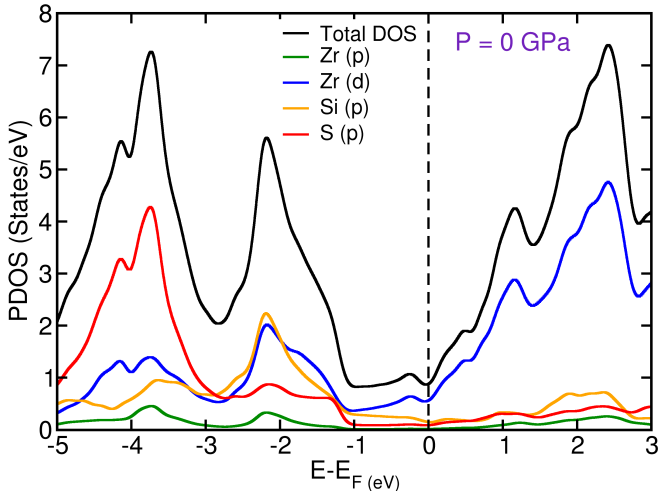

(a)

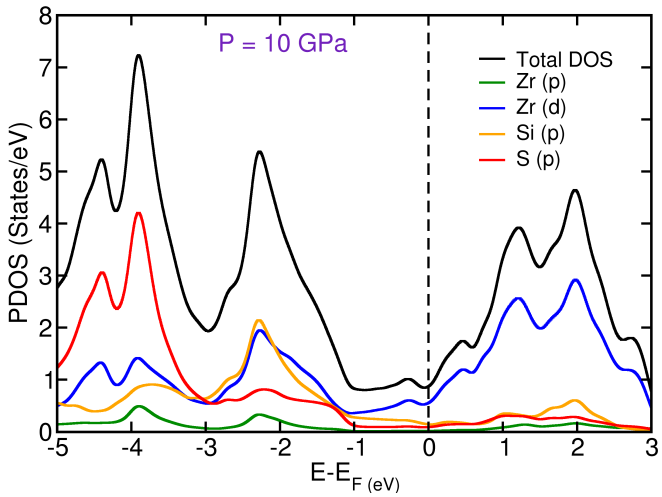

(b)

Figure 2.8: *Projected density of states of the tetragonal phase of ZrSiS (Space group: P4/nmm) at (a) 0 GPa and (b) 10 GPa. Minima at Fermi level indicates the presence of pseudogap. No significant change is observed near Fermi level at 10 GPa.*

The Fig. 2.8 shows *orbital-projected density of states* at 0 and 10 GPa. At Fermi level, Zr-d states contribute maximum electronic states at both pressures. Also, Zr-p states do not contribute electronic states near Fermi level. Above Fermi level, the the states are mostly comprised of vacant Zr-d states. So, it can be understood that Zr atoms are responsible for the high electrical conductivity in ZrSiS. The Si-p and Zr-d states around -2 eV have nearly the same energy, which indicates the strong interaction between the

two. The S-p states have significant contribution near -4 eV, but negligible contribution near Fermi level. Above Fermi level, From Fig. 2.7 and 2.8 it can be observed that drop in DOS above 0.5 eV is due to Zr-d states, as Si and S have very small contribution Fermi level.

2.4.3 Electronic transport

To calculate electronic transport properties we have used the density functional theory based electronic structure and using semi-classical Boltzmann theory which works under the approximation of constant scattering time as implemented in the BoltzTraP code [14].

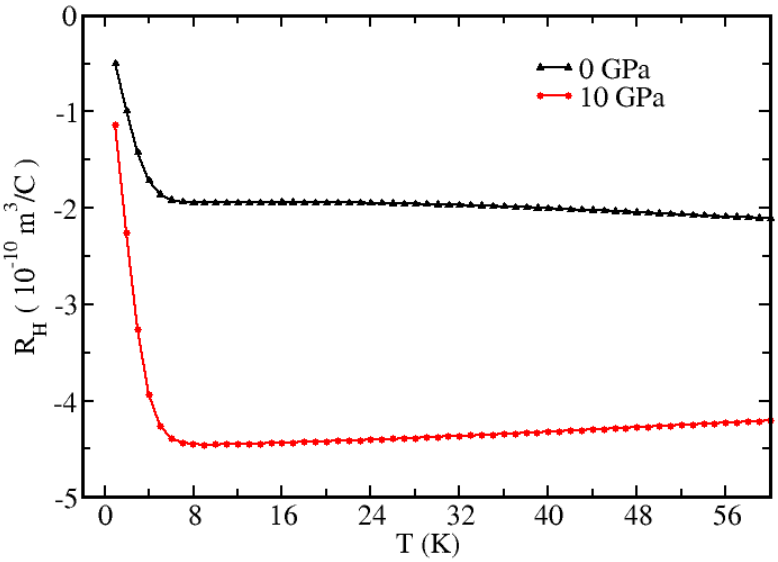

Figure 2.9: *Calculated Hall coeffiecient at 0 and 10 GPa. The sign of the R_H remains negative at both the pressures, which indicates that conduction is mainly facilitated by electrons.*

The calculated value of Hall coefficient, Fig. 2.9, shows negative values at both pressure, which confirms that the electron are major charge carriers. It can also be observed that at both pressures upto 7 K, the R_H decreases sharply and above it becomes nearly constant. The Hall coefficient in the Drude model accounts only for the free electron gas. It does not considers the effect of background potential in the material, such as effect

of the atomic centers or any other applied field. In ZrSiS the value of Hall coefficient is negative unlike other metals such as tungsten, beryllium and cadmium [16] which have a positive hall coefficient. This implies that the electrons are free enough to move around and indicates the normal metallic character in ZrSiS, where the conduction is mainly facilitated by the electrons. However, it was earlier shown by Singha et. al by using the classic two-band model, that both types of carriers i.e. e^- and holes, contribute to the transport. But, at low temperatures the hole mobility is very low as compared to the mobility of electrons.

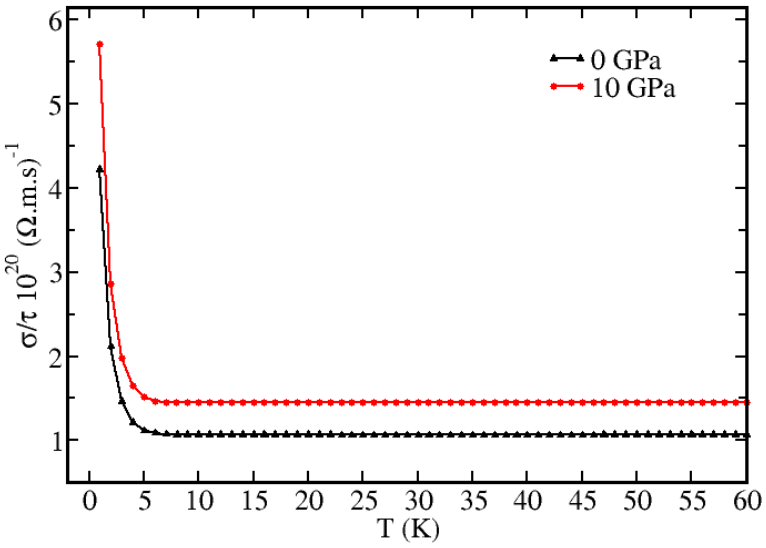

Figure 2.10: *Plots showing conductivity normalized with relaxation time with respect to temperature at 0 and 10 GPa. The conductivity is higher at 10 GPa as compared to 0 GPa.*

In Fig.2.10, the conductivity plots are shown. It can be observed that at low temperatures the conductivity at 10 GPa is high with respect to 0 GPa. This implies that the tetragonal phase is not responsible for the jump in the resistivity. The plot with respect to Fermi level can understood in a way that left side corresponds to p-type and right side to n-type doping. It can be observed that minima is at $E = E_F$. This is obvious because introduction of more charge carriers in the system leads to the increase in conductivity.

2.5 Conclusions

Finally to conclude, in this work I have tried to understand the origin of pressure-induced jump in the resistivity. It can be observed that there is no significant change in the electronic structure of tetragonal phase of ZrSiS under pressure which would have resulted in the unique behaviour of the resistivity. Further, from our conductivity calculations under semi-classical Boltzman transport theory, we have showed that there is an increase in the conductivity of the tetragonal phase. Thus, we can say that the tetragonal phase is not responsible for the observed behaviour of the electronic transport. It is known that there is a structural phase transition from tetragonal to orthorhombic phase under pressure. Singha et al. showed that through the raman scattering measurements that under pressure, an siotropic structure is formed [8]. It is also discussed in the review by Yang et al., that square lattice protects the band crossings [17]. So, it is expected that orthorhombic phase is responsible for the observed jump in the resistivity where the symmetry breaking of the Si-square mesh might be responsible for the anomalous behaviour of the resistivity.

Bibliography

[1] M. Z. Hasan and C. L. Kane, "Colloquium: Topological insulators," *Reviews of modern physics*, vol. 82, no. 4, p. 3045, 2010.

[2] Z. Liu, J. Jiang, B. Zhou, Z. Wang, Y. Zhang, H. Weng, D. Prabhakaran, S. Mo, H. Peng, P. Dudin, *et al.*, "A stable three-dimensional topological Dirac semimetal Cd_3As_2," *Nature materials*, vol. 13, no. 7, p. 677, 2014.

[3] S.-Y. Xu, I. Belopolski, N. Alidoust, M. Neupane, G. Bian, C. Zhang, R. Sankar, G. Chang, Z. Yuan, C.-C. Lee, *et al.*, "Discovery of a Weyl fermion semimetal and topological Fermi arcs," *Science*, vol. 349, no. 6248, pp. 613–617, 2015.

[4] L. M. Schoop, M. N. Ali, C. Straßer, A. Topp, A. Varykhalov, D. Marchenko, V. Duppel, S. S. Parkin, B. V. Lotsch, and C. R. Ast, "Dirac cone protected by non-symmorphic symmetry and three-dimensional Dirac line node in ZrSiS," *Nature communications*, vol. 7, p. 11696, 2016.

[5] A. Klein Haneveld and F. Jellinek, "Zirconium silicide and germanide chalcogenides preparation and crystal structures," *Recueil des Travaux Chimiques des Pays-Bas*, vol. 83, no. 8, pp. 776–783, 1964.

[6] W. Tremel and R. Hoffmann, "Square nets of main-group elements in solid-state materials," *Journal of the American Chemical Society*, vol. 109, no. 1, pp. 124–140, 1987.

[7] W. Zhou, H. Gao, J. Zhang, R. Fang, H. Song, T. Hu, A. Stroppa, L. Li, X. Wang, S. Ruan, *et al.*, "Lattice dynamics of Dirac node-line semimetal ZrSiS," *Physical Review B*, vol. 96, no. 6, p. 064103, 2017.

[8] R. Singha, S. Samanta, S. Chatterjee, A. Pariari, D. Majumdar, B. Satpati, L. Wang, A. Singha, and P. Mandal, "Probing lattice dynamics and electron-phonon coupling in the topological nodal-line semimetal ZrSiS," *Phys. Rev. B*, vol. 97, p. 094112, Mar 2018.

[9] R. Singha, A. K. Pariari, B. Satpati, and P. Mandal, "Large nonsaturating magnetoresistance and signature of nondegenerate Dirac nodes in ZrSiS," *Proceedings of the National Academy of Sciences*, vol. 114, no. 10, pp. 2468–2473, 2017.

[10] P. Giannozzi, S. Baroni, N. Bonini, M. Calandra, R. Car, C. Cavazzoni, D. Ceresoli, G. L. Chiarotti, M. Cococcioni, I. Dabo, A. D. Corso, S. de Gironcoli, S. Fabris, G. Fratesi, R. Gebauer, U. Gerstmann, C. Gougoussis, A. Kokalj, M. Lazzeri, L. Martin-Samos, N. Marzari, F. Mauri, R. Mazzarello, S. Paolini, A. Pasquarello, L. Paulatto, C. Sbraccia, S. Scandolo, G. Sclauzero, A. P. Seitsonen, A. Smogunov,

P. Umari, and R. M. Wentzcovitch, "QUANTUM ESPRESSO: a modular and open-source software project for quantum simulations of materials," *Journal of Physics: Condensed Matter*, vol. 21, p. 395502, sep 2009.

[11] A. D. Corso, "Pseudopotentials periodic table: From H to Pu," *Computational Materials Science*, vol. 95, pp. 337 – 350, 2014.

[12] X. Hua, X. Chen, and W. A. Goddard, "Generalized generalized gradient approximation: An improved density-functional theory for accurate orbital eigenvalues," *Phys. Rev. B*, vol. 55, pp. 16103–16109, Jun 1997.

[13] J. P. Perdew, K. Burke, and M. Ernzerhof, "Generalized gradient approximation made simple," *Phys. Rev. Lett.*, vol. 77, pp. 3865–3868, Oct 1996.

[14] G. K. Madsen and D. J. Singh, "BoltzTraP. A code for calculating band-structure dependent quantities," *Computer Physics Communications*, vol. 175, no. 1, pp. 67–71, 2006.

[15] A. Bera, K. Pal, D. V. S. Muthu, U. V. Waghmare, and A. K. Sood, "Pressure-induced phase transition in Bi_2Se_3 at 3 GPa: Electronic topological transition or not?," *Journal of Physics: Condensed Matter*, vol. 28, p. 105401, feb 2016.

[16] D. E. Gray *et al.*, *American institute of physics handbook*. 1972.

[17] S.-Y. Yang, H. Yang, E. Derunova, S. S. Parkin, B. Yan, and M. N. Ali, "Symmetry demanded topological nodal-line materials," *Advances in Physics: X*, vol. 3, no. 1, p. 1414631, 2018.

Chapter 3

Pressure induced evolution of energy bands and their band widths in PbTe

3.1 Introduction

The energy levels of materials have remained one of the most interesting things to look at as they give insight about how electrons behave. At atomic scale, discrete energy levels are present, whereas in solids these energy levels merge to form energy bands. The interaction between the energy levels depend upon the which orbitals are close in energy, bond angles, interatomic distance, number of valence electrons etc. The space between the atoms is filled by the electrons which act as glue and hold all the atoms together. The electrons which do not take part in bonding, i.e. the electrons in inner completely filled orbitals, generally do not affect the electronic properties of the material. The valence electrons and the unfilled orbitals of atoms determine the electronic band gap of the material. So, any perturbation to the material which affects the energy levels of the material (impurity atoms, defects, temperature, pressure, defects, electric field etc.), is very interesting. These perturbations affect the way in which wave functions overlap and thus affect the electronic properties. This work is motivated by the these concepts. Here,

we tried to understand the effect of pressure on the band width of the electronic energy bands in PbTe. The crystal structure of PbTe at room temperature has rock-salt type structure (Space group: $Fm\bar{3}m$), which has two atoms in the primitive unit cell where each atom has a coordination number of six [1]. It is a promising thermoelectric material with a band gap of 0.32 eV [2].

The properties of materials largely depend on the energy bands and there interactions. The energy bands in solids are forms by the overlap of orbitals. The energy bands due to core states are lower in energy whereas energy bands responsible for the transport properties of the materials are higher in energy. The core states can be tuned by application of the pressure which deforms the energy bands. In this work we have to understand the effect of pressure in the evolution of energy bands in this material. In an earlier work, PbS, PbSe and PbTe were studied and band structure was studied, and they showed the level repulsion between Pb-p and X-s(X = S, Se and Te) orbitals [3, 4], which was found to be maximum in the case of PbS. All three materials have rock-salt structure with a decreasing lattice constant as the size of the chalocogen (X = S, Se and Te) decreases. Thus, to look for any signatures of level repulsion of PbTe under pressure by continuously applying hydrostatic pressure on the system is interesting and fundamentally important. It was also showed that band gap has a negative deformation potential, which means that band gap decreases with respect to increasing hydrostatic pressure. We have tried to understand these aspects in our work under the application of continuous hydrostatic pressure.

3.2 Computational Details

The calculations at various pressures was done using density functional theory as implemented in the Quantum ESPRESSO software package [5]. The ultrasoft pseudopotentials were implemented in our calculations [6]. The exchange-correlation was treated under

generalized gradient approximation (GGA) [7] and the functional form as parameterized by Perdew-Burke-Ernzherof [8]. The energy cutoff for the basis of the plane waves used was 65 Ry and with a cutoff of 650 Ry for charge density. A uniform k-point grid of $24 \times 24 \times 24$ was used for integrations over the Brillouin zone width a smearing width of 0.003 Ry. The structures were optimised at pressures upto 25 GPa under BFGS algorithm untill the forces on all atoms are minimum.

3.3 Results and discussion

The evolution of energy bands can be tracked through the density of states calculations. The density of states helps to understand the nature of the orbitals which are interacting. It also helps to determine which orbitals are forming valence band maxima (VBM) or conduction band minima (CBM). In this work studied the evolution of the energy bands through projected density of states calculations at various pressures. The pressure causes a decrease in the volume and increases the interaction between various energy bands in the material. We have done calculations starting from -2 GPa upto 25 GPa. The negative pressure was applied to check if band widths decrease if volume is increased. The decrease in volume is related to decoupling of interactions between the electronic wave functions. This causes the energy bands to get separated and eventually if we have isolated atoms, the energy bands turn into discrete energy levels.

In the structure of PbTe, the atoms form an octahedra with Pb at the center of octahedra. The increase in pressure causes a decrease in the volume of the octahedra and thus increases the coupling between the p-p orbitals, which is the main reason of the decrease in the band gap of PbTe at higher pressures. In Fig. 3.3, projected density of states are showed. The electronic configuration of Pb is $[Xe]4f^{14}5d^{10}6s^26p^2$ and that of Te is $[Kr]4d^{10}5d^{10}6s^26p^2$.

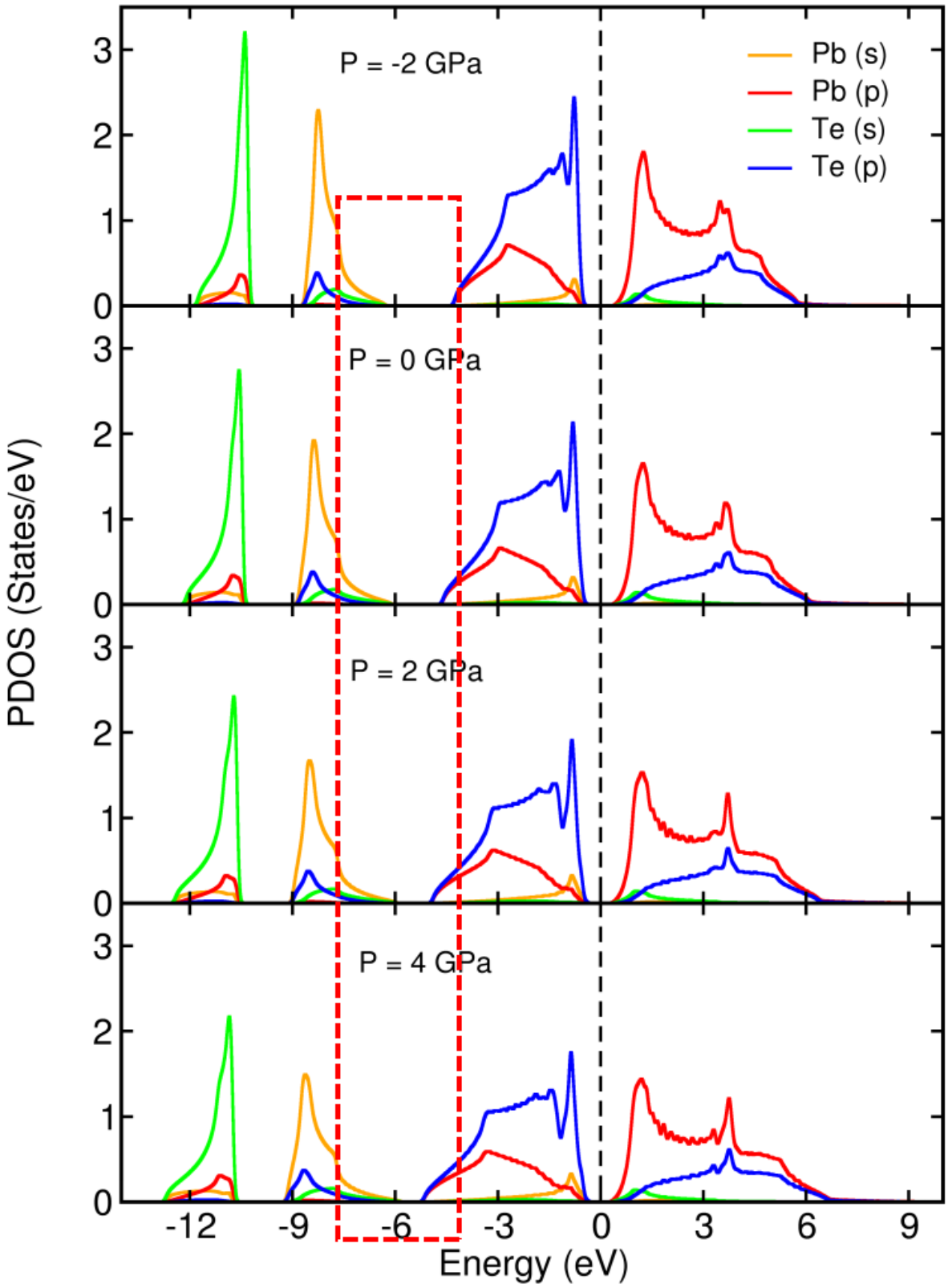

Figure 3.1: *Projected density of states of PbTe. The band width of the energy bands increase with an increasing pressure. The VBM and CBM have contribution largely from Te (5p) and Pb (6s) orbitals respectively.*

It can be observed that contribution to VBM and CBM mainly comes from the Te ($5p$) filled states and Pb ($6p$) vacant states . The partially filled Pb ($6p$) orbitals also contribute slightly to valence band, which can be observed as a broad band below Te ($5p$) in red color. Also, a small peak due to Te ($5p$), below Pb ($6s$), is observed. This shows that there is an interaction between these orbitals. It can also be observed that broadening of the peaks is related to the band width of the energy bands.

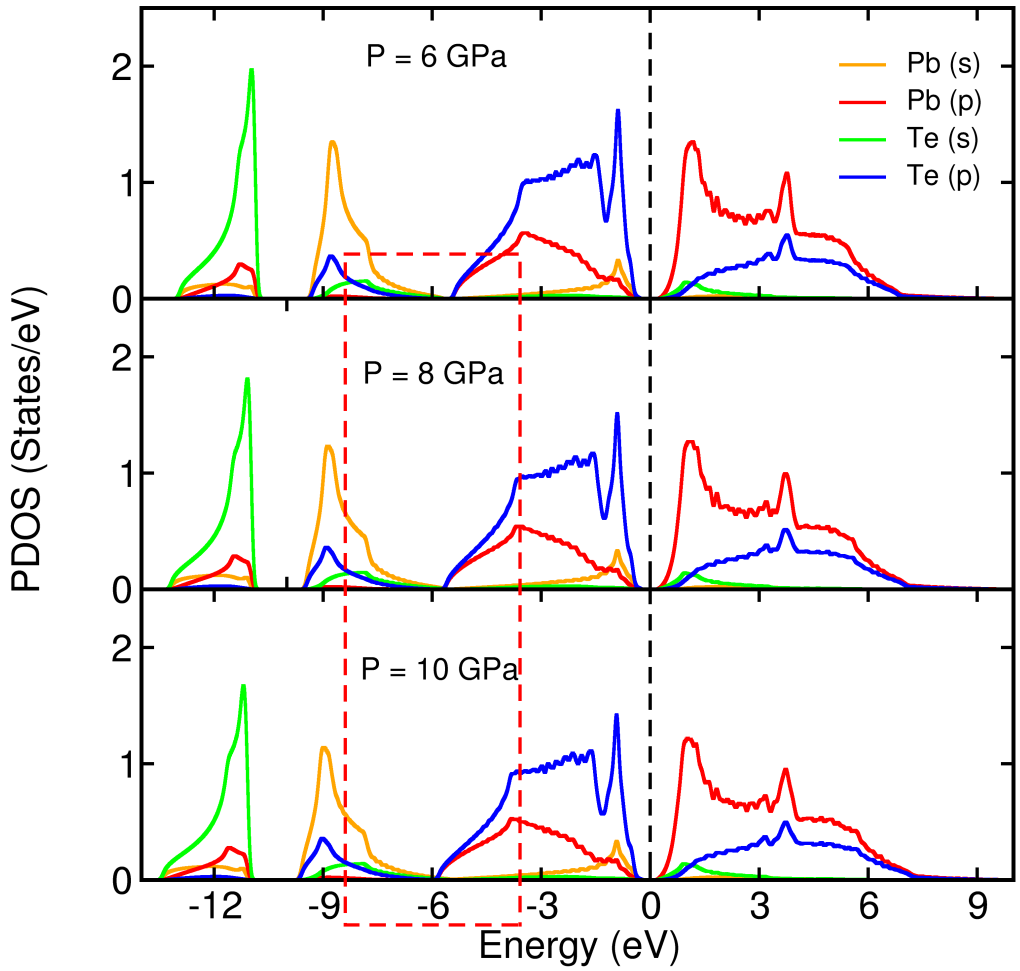

Figure 3.2: *Projected density of states of PbTe . The band width of the energy bands increase with an increasing pressure. It can be observed that energy bands due to Pb (6s) and Te (5p) start to overlap above 8 GPa.*

Above 8 GPa(Fig. 3.3), it was observed that energy bands which have major contributions from Pb ($6s$) and Te ($5p$) start to overlap. There was no level repulsion observed between Pb ($6s$) and Te ($5p$), upon applying a positive pressure.
In Table. 3.1, we have estimated the band widths at various pressures. At -2 GPa, i.e. volume expansion, the band width is minimum for both the cases,. This indicates that upon applying negative pressure, the decoupling between the orbitals is responsible for the decrease of the band width.

Band width of Pb ($6s$) and Te ($5p$) energy bands					
Pressure (GPa)	-2	0	2	4	6
Te ($5p$) (eV)	4.04	4.43	4.82	5.07	5.34
Pb ($6s$) (eV)	2.65	2.95	3.24	3.50	3.79

Table 3.1: *Estimated band widths of the Pb (6s) and Te (5p) energy bands for various pressures. At negative pressure the band width is minimum due to decreased interactions between the orbitals. As the pressure increases, the band width also increases for both orbitals.*

Next we tried to understand the behavior at higher much higher pressures. At 18 GPa, the VBM and CBM start to overlap. This corresponds to strong p-p orbital interactions, due to decrease in volume of the octahedra as the Te atoms come closer to the Pb atom. At 18 GPa, there is significant overlap between Pb ($6s$) and Te ($5p$) orbital, which is clearly visible in Fig. 3.3. It should be noted that, the effect of spin-orbit coupling is not included in the calculations which has significant effect on the electronic properties of materials which have heavy elements. When a system is subjected to high pressures, the orbitals come closer to each other and thus, effect of spin-orbit coupling becomes very important.

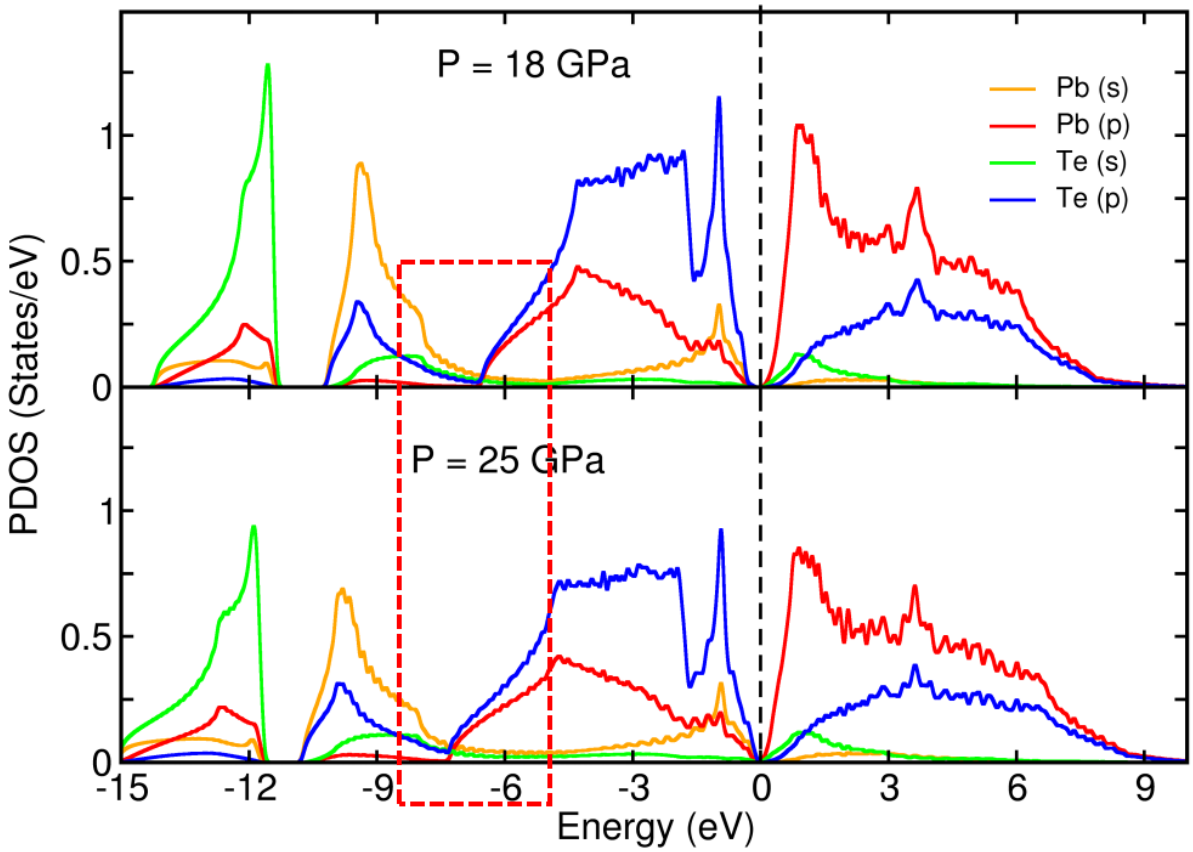

Figure 3.3: *Projected density of states of PbTe. The valence band maximum (VBM) and conduction band minimum (CBM) overlap at 18 GPa. There is no level repulsion observed between Pb (6s) and Te (5p) even at higher pressures.*

It should also be noted that band width continuously increases with pressure. The broadening can be related to the delocalization of the electronic states due to increased scattering processes at high pressures. In Fig. 3.3, a schematic is shown for the calculations done in this work. It can observed that Pb ($6p$) does not interacts with the Te ($5p$) even at high pressures. But at high pressures, the vacant Pb ($6p$) in CBM start to overlap with Te ($5p$) and thus band gap decreases to zero. The Te ($5s$) states are very low in energy, but even then the pressure causes an increase in the band width of these states. The band width of the Te ($5s$) increases with pressure but it does not interacts with the

Pb ($6s$) orbital. The energy gap between these two orbitals decreases with pressure but they do not overlap even at 25 GPa.

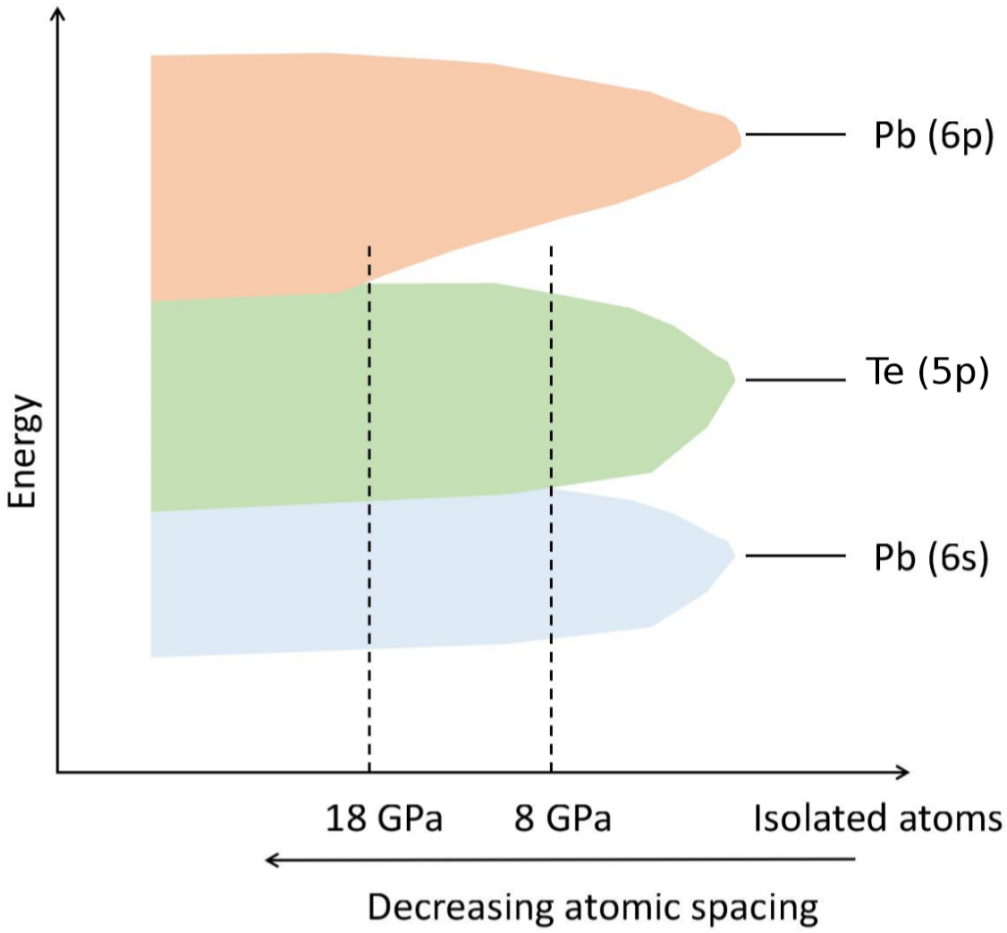

Figure 3.4: *Schematic of evolution of energy bands of PbTe under pressure. At 8GPa the Pb (6s) and Te (5p) orbitals overlap and above 18 GPa the VBM and CBM start to touch each other and continues upto 25 GPa.*

Fig.3.3 shows the schematic of evolution of the energy bands of PbTe under pressure. The effect of pressure causes the bands to merge. The VBM and CBM start to merge around 18 GPa, whereas Te ($5p$) and Pb ($6s$) bands merge at 8 GPa.

3.4 Conclusion

In this work I have tried to study the role of pressure on energy bands of PbTe. It was clearly demonstrated that band width of each energy bands increases with as the value of hydrostatic pressure applied on the system increases. This causes the closing of band gap as well as merging of Pb ($6s$) and Te ($5p$) states. It was also observed that band width of Te ($5s$) energy band also increases but the the gap between Te ($5s$) and Pb ($6s$) sustains upto 25 GPa. The effect of spin-orbit coupling is not included which is interesting to look at as the pressure increases.

Bibliography

[1] Y. Noda, S. Ohba, S. Sato, and Y. Saito, "Charge distribution and atomic thermal vibration in lead chalcogenide crystals," *Acta Crystallographica Section B: Structural Science*, vol. 39, no. 3, pp. 312–317, 1983.

[2] M. G. Kanatzidis, "Nanostructured thermoelectrics: The new paradigm?," *Chemistry of Materials*, vol. 22, no. 3, pp. 648–659, 2010.

[3] S.-H. Wei and A. Zunger, "Electronic and structural anomalies in lead chalcogenides," *Physical Review B*, vol. 55, no. 20, p. 13605, 1997.

[4] Y.-H. Li, X. Gong, and S.-H. Wei, "Ab initio all-electron calculation of absolute volume deformation potentials of iv-iv, iii-v, and ii-vi semiconductors: The chemical trends," *Physical Review B*, vol. 73, no. 24, p. 245206, 2006.

[5] P. Giannozzi, S. Baroni, N. Bonini, M. Calandra, R. Car, C. Cavazzoni, D. Ceresoli, G. L. Chiarotti, M. Cococcioni, I. Dabo, A. D. Corso, S. de Gironcoli, S. Fabris, G. Fratesi, R. Gebauer, U. Gerstmann, C. Gougoussis, A. Kokalj, M. Lazzeri, L. Martin-Samos, N. Marzari, F. Mauri, R. Mazzarello, S. Paolini, A. Pasquarello,

L. Paulatto, C. Sbraccia, S. Scandolo, G. Sclauzero, A. P. Seitsonen, A. Smogunov, P. Umari, and R. M. Wentzcovitch, "QUANTUM ESPRESSO: a modular and open-source software project for quantum simulations of materials," *Journal of Physics: Condensed Matter*, vol. 21, p. 395502, sep 2009.

[6] A. D. Corso, "Pseudopotentials periodic table: From h to pu," *Computational Materials Science*, vol. 95, pp. 337 – 350, 2014.

[7] X. Hua, X. Chen, and W. A. Goddard, "Generalized generalized gradient approximation:an improved density-functional theory for accurate orbital eigenvalues," *Phys. Rev. B*, vol. 55, pp. 16103–16109, Jun 1997.

[8] J. P. Perdew, K. Burke, and M. Ernzerhof, "Generalized gradient approximation made simple," *Phys. Rev. Lett.*, vol. 77, pp. 3865–3868, Oct 1996.